

CASE FILE  
COPY

NASA

*10-24*  
*1959*

# MEMORANDUM

COMPRESSIVE STRENGTH OF STAINLESS-STEEL  
SANDWICHES AT ELEVATED TEMPERATURES

By Eldon E. Mathauser and Richard A. Pride

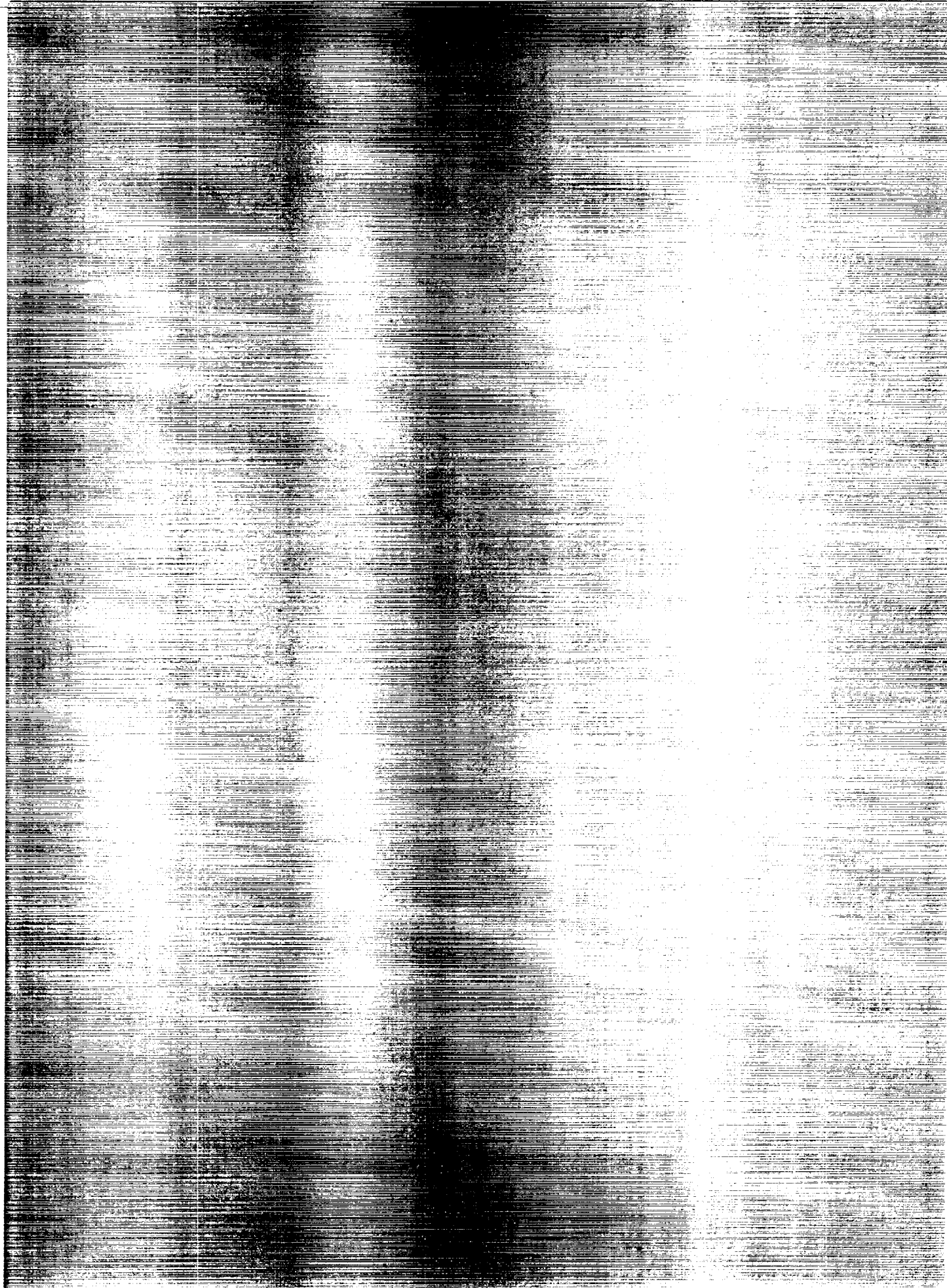
Langley Research Center  
Langley Field, Va.

NATIONAL AERONAUTICS AND  
SPACE ADMINISTRATION

WASHINGTON

June 1959

NASA MEMO 6-2-59L



NATIONAL AERONAUTICS AND SPACE ADMINISTRATION

---

MEMORANDUM 6-2-59L

---

COMPRESSIVE STRENGTH OF STAINLESS-STEEL

SANDWICHES AT ELEVATED TEMPERATURES

By Eldon E. Mathauser and Richard A. Pride

SUMMARY

Experimental results are presented from crippling tests of stainless-steel sandwich specimens in the temperature range from 80° F to 1,200° F. The specimens included resistance-welded 17-7 PH stainless-steel sandwiches with single-corrugated cores, type 301 stainless-steel sandwiches with double-corrugated cores, and brazed 17-7 PH stainless-steel sandwiches with honeycomb cores. The experimental strengths are compared with predicted buckling and crippling strengths. The crippling strengths were predicted from the calculated maximum strength of the individual plate elements of the sandwiches and from a correlation procedure which gives the elevated-temperature crippling strength when the experimental room-temperature crippling strengths are known. Photographs of some of the tested specimens are included to show the modes of failure.

INTRODUCTION

The requirements for high strength, stiffness, and light weight in flight structures fabricated from heat-resistant materials have produced increasing interest in sandwich plate construction. Two types of sandwich plate construction of current interest are the honeycomb-core and the corrugated-core types. To date, very little information is available on the strength of either type at temperatures that are above the range for adhesive bonding. The results of some tests on brazed honeycomb-core stainless-steel sandwiches up to 1,200° F are available in reference 1. Reference 2 presents some results obtained from crippling tests of corrugated-core sandwiches at room temperature; however, no results of tests made at elevated temperatures are given. The present study was made to obtain experimental strength data on both types of sandwich plate constructions in the temperature range from 80° F to 1,200° F.

The sandwiches tested in the present investigation were resistance-welded specimens of 17-7 PH and type 301 stainless steel with single- and double-corrugated cores and brazed 17-7 PH stainless-steel specimens with hexagonal- and square-cell honeycomb cores. The sandwich specimens

were tested in axial compression without side support to determine the maximum or crippling strengths and modes of failure. The buckling and crippling strengths of the sandwiches were predicted on the basis of existing methods and are compared with the experimental results. A materials correlation parameter is investigated for predicting the elevated-temperature crippling strength of the sandwiches from the experimental room-temperature crippling strength.

#### SYMBOLS

$b$	width of plate element, in.
$b_c$	width of plate element in core, in.
$b_f$	width of plate element in face sheet, in.
$E$	modulus of elasticity, ksi
$E_s$	secant modulus, ksi
$E_t$	tangent modulus, ksi
$G$	shear modulus of elasticity, ksi
$G_c$	shear modulus of core, ksi
$h$	overall thickness of sandwich plate, in.
$h_c$	thickness (height) of core, in.
$k$	compressive buckling coefficient
$L$	length, in.
$P_{cr}$	buckling load, kips
$t$	thickness of plate element, in.
$t_c$	thickness of core element, in.
$t_f$	thickness of face sheet, in.
$T$	temperature, $^{\circ}F$

$w$	overall width of sandwich face, in.
$\epsilon$	strain
$\bar{\epsilon}$	unit shortening
$\bar{\epsilon}_f$	unit shortening at maximum (crippling) load
$\mu$	Poisson's ratio
$\rho_c$	effective core density, lb/cu in.
$\rho_f$	facing-material density, lb/cu in.
$\sigma$	stress, ksi
$\bar{\sigma}$	average stress, ksi
$\sigma_{cr}$	buckling (critical) stress, ksi
$\bar{\sigma}_{cr}$	average buckling (critical) stress for sandwich, ksi
$\sigma_{cy}$	0.2-percent-offset compressive-yield stress, ksi
$\bar{\sigma}_f$	average stress at maximum (crippling) load, ksi
$\tau_c$	effective shear stress in core, ksi
$\gamma$	shear strain
$\eta$	plasticity reduction factor

## SPECIMENS, EQUIPMENT, AND PROCEDURES

### Specimens

The specimens tested in the present investigation consisted of resistance-welded 17-7 PH and type 301 stainless-steel sandwiches with single- and double-corrugated cores and brazed 17-7 PH stainless-steel sandwiches with hexagonal- and square-cell honeycomb cores. The resistance-welded sandwiches were fabricated by The Budd Company, Philadelphia, Pennsylvania, and the brazed honeycomb-core sandwiches by The Martin Company, Baltimore, Maryland. The test specimens were

approximately 2.2 inches wide and either 2.0 or 2.5 inches long. All specimens were cut from sandwich panels approximately 2 feet square and then machined to final dimensions. The specimen sizes, material thicknesses, heat-treat conditions, and other related data are given in figure 1.

Corrugated-core sandwiches.- The resistance-welded corrugated-core sandwiches consisted of specimens with single- and double-corrugated cores. The specimens with single-corrugated cores were fabricated from 17-7 PH stainless steel and were heat treated to a material strength representative of Condition TH 1,050. The specimens included the sandwiches with equal-thickness face sheets shown in figure 1(a) and the sandwiches with unequal-thickness face sheets shown in figure 1(b). Both of these types of specimens with single-corrugated cores weighed 2 pounds per square foot.

The sandwich specimens with double-corrugated cores were fabricated from stress-relieved type 301 stainless steel with extra-hard temper material in the face sheets and full-hard temper or corrugating temper material in the cores. The specimens with double-corrugated cores included the sandwiches weighing 1 pound per square foot shown in figure 1(c) and the sandwiches weighing 2 pounds per square foot shown in figure 1(d).

The sandwiches with corrugated cores were fabricated by spotwelding the face sheets to the preformed corrugated cores. These spot welds were closely spaced to produce essentially continuous welds between the face sheets and the cores.

Honeycomb-core sandwiches.- Two types of honeycomb-core sandwiches were included in the present investigation. One type, which is shown in figure 1(e), consisted of brazed square-cell honeycomb-core sandwiches made of 17-7 PH stainless-steel face sheets and type 321 stainless-steel cores. The other type, which is shown in figure 1(f), consisted of brazed hexagonal-cell honeycomb-core sandwiches with both face sheets and cores of 17-7 PH stainless steel. Both types of sandwiches were heat treated at 1,125° F after brazing. The square-cell honeycomb-core specimens weighed 3.4 pounds per square foot, and the hexagonal-cell honeycomb-core specimens weighed 3.1 pounds per square foot. The square-cell honeycomb-core specimens were loaded in the direction of the core ribbons, and the hexagonal-cell honeycomb-core specimens were loaded in a direction perpendicular to the core ribbons.

#### Equipment and Procedures

Axial compressive loads were applied on the specimens by means of a 120,000-pound-capacity universal hydraulic testing machine. The

specimens were machined with ends flat and parallel and were supported directly on the loading ram without any end fixture or side reinforcement. Unit shortening was measured over a 1-inch gage length at the midheight of each specimen (see fig. 2) and was recorded autographically against applied load.

The sandwich specimens were heated to test temperature in an oven supported in the testing machine. Both the upper and the lower rams through which the load was applied on the specimens were heated to aid in maintaining uniform specimen temperature.

The temperature of the specimens was determined with the aid of an automatic temperature recorder in conjunction with chromel-alumel thermocouples spotwelded to the specimens. One thermocouple was spotwelded on the sandwich specimen at the center of one face sheet, and three additional thermocouples were spotwelded on the other face sheet on a line passing through the diagonal corners of the face sheet. One of these three thermocouples was located at the midheight and the other two approximately  $1/4$  inch from the corners.

In the elevated-temperature tests, the specimens with extensometer attached were placed into the oven that had been preheated to test temperature. The specimens were exposed to test temperature for thirty minutes and then loaded at a nominal rate of unit shortening of 0.005 per minute until maximum load was obtained. During loading the temperatures of the specimens were maintained within  $\pm 5^{\circ}$  F of the test temperatures shown in table I. The exposure temperatures prior to loading were maintained within  $\pm 5^{\circ}$  F of the reported test temperatures with infrequent variation of  $\pm 10^{\circ}$  F during the initial portion of the 30-minute exposure period.

In addition to the axial compression tests, shear tests were made on the honeycomb-core specimens at room temperature to determine the shear moduli of the cores. A view of the specimen assembly prepared for these tests is shown in figure 3. Two nominally identical sandwich specimens were adhesively bonded to a single strip of  $\frac{1}{8}$ -inch-thick

aluminum alloy. Two additional strips of  $\frac{1}{16}$ -inch-thick aluminum alloy

were then bonded to the outer faces of the sandwich specimens to form the assembly shown in figure 3. This assembly was subjected to a tensile load in a 120,000-pound-capacity universal hydraulic testing machine as shown in figure 4. Tuckerman optical strain gages with modified knife edges were mounted on each side of this assembly (see fig. 4) and were used to measure the relative motion between the face sheets of each sandwich specimen in the direction of loading. The strain gages were read at small increments of load until maximum load was obtained. The relative motion of the face sheets measured over the length of the

specimens in the direction of loading (see fig. 3) was used to establish the magnitude of the overall shear deformation of the cores. The data obtained from these tests are given subsequently in the discussion on the test results for the honeycomb-core sandwiches.

Compressive stress-strain tests were made on specimens obtained from the face sheets of the honeycomb-core panels. These specimens were prepared by removing the core and brazing material from the face sheets by machining. The finished compressive stress-strain specimens were 1.00 inch wide and 2.52 inches long. These specimens were exposed for 30 minutes at the elevated test temperature and then loaded at a nominal strain rate of 0.005 per minute. The test procedure for these stress-strain tests was similar to that described in reference 3.

## RESULTS AND DISCUSSION

The experimental results of the present investigation are given in the following sections, and comparisons with predicted results are included. The maximum strengths of the sandwich specimens determined from the axial compression test (table I) and predicted buckling and maximum strengths are given in part (a) of figures 5 to 10. The axial deformations of the sandwiches under compressive loading are shown in the experimental curves of average stress plotted against unit shortening in part (b) of figures 5 to 10. The buckle patterns and failure modes are shown in photographs of the tested specimens in part (c) of figures 5 to 10 and in figure 6(d). Figures 11 to 13 are included to show compressive stress-strain data for the sandwich materials over the range of test temperatures. Brief descriptions of the methods employed to predict buckling and maximum strengths are given in appendixes A to D.

### Single-Corrugated-Core Sandwich Specimens

The maximum experimental strengths of the sandwiches with single-corrugated cores for the range from room temperature to 1,200° F are indicated by the symbols in figures 5(a) and 6(a). The nominal cross-sectional areas of both types of specimens were the same, and approximately similar strengths were obtained with both types of specimens at the same test temperatures. No evidence of column bending was discernible in the specimens. The maximum strengths were thus assumed to be indicative of the crippling strengths of the sandwiches. The maximum strengths showed an expected decrease with increasing temperatures. Some scatter in the test data was obtained, particularly for the specimens with equal-thickness face sheets. (See, for example, fig. 5(a).) This scatter may be the result of variations in material properties, variations in material thicknesses from the nominal gages, variation in



fabrication techniques, the presence of small eccentricities in the specimens, and possible misalignment between the specimens and the loading surfaces. Observation of the test specimens indicated that the resistance welds were adequate and did not contribute to the test scatter.

The solid curves shown in figures 5(a) and 6(a) indicate the predicted maximum strengths obtained from a summation of the maximum strengths of the plate elements. The dot-dash curves shown in the same figures indicate the maximum strengths obtained from the correlation procedure described in appendix B and shown in figure 14. The predicted strengths determined from the correlation procedure are generally in closer agreement with the experimental data than the predictions obtained from the summation of the maximum strength of the plate elements. It may be noted, however, that the experimental room-temperature crippling strength is required in order to make use of the correlation procedure.

Some of the deviations between the experimental and predicted strengths may be attributed to inadequate knowledge of the mechanical properties of the sheet material in the sandwiches. The material stress-strain curves (fig. 11) which were used to predict maximum strength were obtained from tests of material having a thicker gage than that used in the sandwiches. The thin-gage material used in the specimens was not amenable for use in compression stress-strain tests in the existing facilities. Furthermore, no study was made to determine if the mechanical properties of the thin sheet were altered by the resistance welding.

The dotted curve shown in figure 6(a) indicates the predicted local buckling stresses (see appendix A). The comparable curve in figure 5(a) is coincident with the maximum-strength curve. A comparison between the experimental and theoretical buckling stresses is not included because experimental values of the local buckling stresses were not obtained. Approximate values of the experimental local buckling stresses can be estimated from the curves of average stress plotted against unit shortening shown in figures 5(b) and 6(b). The local buckling stresses are defined by the initial deviation of the curves of average stress against unit shortening from the corresponding material stress-strain curves shown in figure 11.

For the sandwich specimens having face sheets of equal thickness, buckling of both face sheets is anticipated on the basis of the buckling theory for corrugated-core sandwiches presented in reference 4. For the specimens with face sheets of unequal thickness, the core and the thinner face sheet are predicted to buckle at the stresses indicated in figure 6(a), and the thicker face sheet is expected to remain flat. The results of the tests on both types of sandwich specimens generally substantiate the predicted modes of buckling. In figure 5(c) the buckle pattern obtained at the low test temperature (208° F) consisted of local

buckles over both faces of the specimens. Most of the local buckles are not discernible in the unloaded specimen shown in figure 5(c), with the exception of a single line of local buckles. These buckles extend across each face of the specimen and define the region of local failure. The local buckles that formed in each face at the high test temperature (996° F) shown in specimen 11 remained in the specimen upon unloading.

For the specimens with face sheets of unequal thickness, the buckle pattern that was produced in the thinner face is indicated in figure 6(c). Local buckles are also shown in the thicker face of the same specimen in figure 6(d); however, it is believed that these buckles were formed when the specimen was loaded beyond buckling in order to establish maximum strength. Only a slight evidence of local buckles appears in the thicker face of specimen 23 in figure 6(d) in contrast to the deep buckles shown in the thinner face of the same specimen in figure 6(c).

#### Double-Corrugated-Core Sandwich Specimens

The maximum experimental strengths ranging from room temperature to 1,200° F are indicated by the symbols in figure 7(a) for the specimens weighing 1 pound per square foot and in figure 8(a) for the specimens weighing 2 pounds per square foot. The experimental strengths were assumed to be indicative of the crippling strengths of the sandwiches inasmuch as no evidence of column bending was obtained. These experimental results exhibit scatter comparable to that obtained with the specimens with single-corrugated cores. Variations in material properties may have contributed to this test scatter. The tempers of the type 301 stainless steel from which the sandwiches were fabricated (see fig. 12 and table II) are considered to be in the developmental stage and, consequently, variations in mechanical properties may have existed in the sheet materials. Visual observation of the specimens indicated that the resistance welds were satisfactory and did not contribute to the test scatter.

The predicted maximum strengths determined from a summation of the maximum strength of the plate elements of the sandwich and from the correlation procedure are indicated by the solid and dot-dash curves, respectively, in figures 7(a) and 8(a). The strengths predicted from the correlation procedure are in better agreement with the experimental data, particularly for the results shown in figure 8(a) for the 2-pounds-per-square-foot sandwich. The dotted curves shown in figures 7(a) and 8(a) indicate the predicted local buckling stresses. The buckling and maximum strengths for both types of sandwiches with double-corrugated cores were obtained with the aid of the material stress-strain curves shown in figure 12. These curves were assumed to be adequately representative of the material properties in both sandwiches for purposes of this analysis. It may be noted that the room-temperature yield

stress values which were submitted by the fabricator and reported to be appropriate to the material in the 1-pound-per-square-foot sandwich were in better agreement with the data in figure 12 than the yield stress values submitted as representative of the material in the 2-pounds-per-square-foot sandwich.

Because of the significant differences in the longitudinal and transverse material properties, effective stress-strain curves (appendix D) were used in calculating both buckling and maximum strengths. The effective stress-strain curves represent a weighted average of the longitudinal and transverse properties. The material stress-strain curves corresponding to the loading direction of the sandwich were weighted twice as heavily as the stress-strain curves transverse to the loading direction in order to obtain the effective stress-strain curve for each temper.

The failure modes shown in figures 7(c) and 8(c) were anticipated on the basis of the buckling theory of reference 4. The failure mode shown in figure 7(c) occurs when the face sheets are the destabilizing elements and is characterized by the formation of many local buckles in the face sheets. Maximum strengths predicted for this failure mode on the basis of equation (B1) given in appendix B show good agreement with the experimental maximum strengths shown in figure 7(a). A contrasting mode of failure, shown in figure 8(c) is produced when the core is the destabilizing element. Failure occurs when the core buckles and destabilizes the face sheets and thus produces a wrinkle across the face sheets. Maximum strength predicted for this failure mode on the basis of equation (B1) does not show good agreement with the experimental maximum strength shown in figure 8(a).

#### Honeycomb-Core Sandwiches

The experimental maximum strengths obtained from the square-cell and hexagonal-cell honeycomb-core specimens are shown in figures 9(a) and 10(a), respectively, for the range from room temperature to 1,200° F. These specimens were fabricated primarily for investigating brazing methods and were not designed to yield structurally efficient specimens. The sandwiches contained relatively lightweight cores and thick face sheets and showed considerably more scatter in maximum strengths than was obtained with sandwich specimens of either the single- or double-corrugated cores. The scatter in test results was anticipated since the results given in reference 2 indicate that core densities comparable to those used in the present honeycomb-core sandwiches will give experimental strengths which may often be less than the predicted strengths. Failure of the sandwich specimens was predicted to occur in a column mode, and it was expected that the high potential strength of the face sheets would not be realized, particularly at the lower test

temperatures. The test results substantiate this prediction. It is of interest to note that the square-cell and the hexagonal-cell cores comprised approximately 13 percent and 9 percent, respectively, of the total weight of materials in the sandwiches. Respective values for the sandwiches with single- and double-corrugated cores ranged from 38 percent to 60 percent.

The predicted strengths of the honeycomb-core specimens are indicated by the curves in figures 9(a) and 10(a). These curves were determined from a relation given in reference 5 which defines the buckling strength of a sandwich plate column and includes the effect of the shear modulus of the core on the buckling strength (see appendix C). No attempt was made to predict the maximum strengths on the basis of a correlation procedure because of the substantial scatter obtained in the test data. In addition, the materials parameter utilized in the correlation procedure for the sandwiches with single- and double-corrugated cores is applicable only when failure occurs by local buckling or crippling. Failure of the honeycomb-core specimens occurred in a column bending mode.

The column failure mode for the square-cell and hexagonal-cell honeycomb-core specimens is shown in figures 9(c) and 10(c), respectively. The unit shortening achieved at maximum load ranged from approximately 0.4 percent to 0.6 percent for test temperatures up to 1,000° F. At higher test temperatures, larger values of unit shortening were obtained. Specimen 70, for example, was tested at approximately 1,200° F and achieved a unit shortening of 4.4 percent at maximum load. These results indicate that the core provided sufficient stabilization of the face sheets at the high temperatures and, therefore, the potential strength of the face sheets was achieved. At low test temperatures, the strengths of the sandwich specimens were influenced heavily by shear deflections of the core, and the high potential strengths of the face sheets were not achieved.

All of the honeycomb-core sandwiches appeared to be brazed satisfactorily. The scatter in the test data shown in figures 9(a) and 10(a) was not attributed to inadequate brazing.

#### CONCLUDING REMARKS

The experimental maximum strengths obtained from small stainless-steel sandwich crippling specimens are presented for the range from room temperature to 1,200° F. The specimens included resistance-welded 17-7 PH stainless-steel sandwiches with single-corrugated cores, type 301 stainless-steel sandwiches with double-corrugated cores, and brazed 17-7 PH stainless-steel sandwiches with honeycomb cores.

The predicted crippling strengths and the expected modes of failure are generally in good agreement with the experimental results for the corrugated-core sandwiches. The elevated-temperature crippling strengths predicted on the basis of correlation procedure show better agreement with the experimental data than strengths obtained from a summation of the maximum strength of the plate elements in the sandwiches. Better agreement was anticipated from the correlation procedure because the elevated-temperature strengths are determined from a knowledge of the experimental room-temperature strength. Moderate scatter in the test results was obtained with these specimens. The resistance welds appeared to be satisfactory and were assumed not to contribute to the scatter that was obtained in the test data.

The experimental strengths of the brazed honeycomb-core specimens exhibited considerably more scatter of the test data than was obtained with the resistance-welded corrugated-core specimens. This scatter was anticipated because of the unbalanced design of the honeycomb-core sandwiches. These specimens were fabricated with thick face sheets and relatively lightweight cores. The predicted strengths of the honeycomb-core specimens are generally only in fair agreement with the test results. The quality of the brazing appeared to be satisfactory and was not considered to be a factor in the scatter that was obtained in the test data.

Langley Research Center,  
National Aeronautics and Space Administration,  
Langley Field, Va., March 4, 1959.

## APPENDIX A

## LOCAL BUCKLING STRESSES FOR CORRUGATED-CORE SANDWICHES

The local buckling stresses for the corrugated-core sandwiches were determined from the equation

$$\sigma_{cr} = \frac{k\pi^2\eta E}{12(1 - \mu^2)} \left( \frac{t_f}{b_f} \right)^2 \quad (A1)$$

where the compressive buckling coefficient  $k$  was determined from reference 4. The plasticity reduction factor  $\eta$  was obtained from the following relation (see ref. 6):

$$\eta = \frac{E_s}{E} \left( \frac{1}{2} + \frac{1}{2} \sqrt{\frac{1}{4} + \frac{3}{4} \frac{E_t}{E_s}} \right) \quad (A2)$$

Equation (A1) can be applied directly when the same material stress-strain properties exist in the face sheets and the core. In the present investigation it was assumed that the same material properties existed in the face sheets and the cores of the single-corrugated-core sandwiches of 17-7 PH stainless steel.

For the double-corrugated-core sandwiches fabricated from type 301 stainless steel, considerably different material properties existed in the face sheets and the cores. Local buckling stresses for these type 301 stainless-steel sandwiches were computed with the aid of effective stress-strain curves. (See appendix D.) The local buckling stress was first established for the destabilizing element in the sandwich. The destabilizing element was defined from the buckling analysis presented in reference 4. If the face sheet was the destabilizing element, equation (A1) was used to determine the local buckling stress from the effective stress-strain curve for the face sheet. The buckling strain corresponding to this predicted buckling stress was then obtained from the material stress-strain curve which corresponded with the loading direction of the face sheet. This buckling strain was then used to determine the buckling stress for the core from the material stress-strain curve appropriate for the loading direction of the core. The average buckling stress for the sandwich  $\bar{\sigma}_{cr}$  was obtained by weighting  $\sigma_{cr}$  for the face sheet and  $\sigma_{cr}$  for the core according to the areas of these elements.

If the core was the destabilizing element, the buckling stress for this element was obtained from the effective stress-strain curve for the core by rewriting equation (A1) as follows:

$$\sigma_{cr} = \frac{k_c \pi^2 \eta E}{12(1 - \mu^2)} \left( \frac{t_c}{b_c} \right)^2 \quad (A3)$$

where the compressive buckling coefficient for the core  $k_c$  was evaluated from the relation

$$k_c = k \frac{\left( \frac{t_f}{b_f} \right)^2}{\left( \frac{t_c}{b_c} \right)^2} \quad (A4)$$

The average buckling stress  $\bar{\sigma}_{cr}$  was obtained, as explained previously, with the role of the face sheet and the core interchanged.

## APPENDIX B

## MAXIMUM (CRIPPLING) STRESSES FOR CORRUGATED-CORE SANDWICHES

## Crippling Stresses Obtained From Strength of Plate Elements

The maximum or crippling strengths of the corrugated-core sandwiches shown by the solid lines in part (a) of figures 5 to 8 were determined from the sum of the strength of the plate elements of the sandwich. The maximum strength of each plate element was obtained from the following equation given in reference 7:

$$\bar{\sigma}_f = 1.60 \sqrt{E_s \sigma_{cy}} \frac{t}{b} \quad (B1)$$

where  $E_s$  is the secant modulus determined from the material stress-strain curve at the stress  $\bar{\sigma}_f$ . The use of this equation, in general, yields stresses that exceed the predicted local buckling stresses determined from equation (A1). In some cases, if local buckling occurs in the plastic range of the material, the computed value of  $\sigma_{cr}$  may exceed slightly the computed value of  $\bar{\sigma}_f$ . This result was obtained for the sandwich specimens as shown in figure 5(a). For this case the crippling stress for the sandwich was taken to be the computed value of  $\sigma_{cr}$  obtained from equation (A1).

In applying equation (B1) to determine maximum strength of the corrugated-core sandwiches fabricated from type 301 stainless steel, different material stress-strain curves were appropriate for the face sheet and for the core. The material properties  $E_s$  and  $\sigma_{cy}$  in this case were evaluated from the effective stress-strain curves for the face sheets and for the core.

## Crippling Stresses Determined From Correlation Procedure

The crippling stresses of the corrugated-core sandwiches shown by the dot-dash lines in part (a) of figures 5 to 8 were obtained from a correlation procedure which is described in reference 7. This procedure is useful for establishing the elevated-temperature strengths when the room-temperature experimental strength is known. Use is made of the



materials parameter  $\sqrt{E_s \sigma_{cy}}$  to predict the effect of a change in material properties on the strength of the sandwich. Reference 7 indicates that a plate assembly will fail at a constant value of  $\frac{\sigma}{\sqrt{E_s \sigma_{cy}}}$  at both room and elevated temperatures. Consequently, if a plot of the variation of  $\frac{\sigma}{\sqrt{E_s \sigma_{cy}}}$  with  $\sigma$  is obtained from the compressive stress-strain curves at room and elevated temperatures, the strength of the sandwich at elevated temperatures can be estimated readily if the room-temperature strength is known.

The plots shown in figure 14 were prepared in order to determine the elevated-temperature crippling stresses from this correlation procedure. Figure 14(a) was prepared from the material stress-strain curves given in figure 11, and figures 14(b) and 14(c) were prepared from representative stress-strain curves for the type 301 stainless-steel sandwiches obtained from figure 12. The representative stress-strain curves were obtained by weighting the effective stress-strain curves for the face sheets and the core in proportion to the amount of face and core material existing in the sandwiches. The dotted lines shown in figure 14 indicate a constant value of the parameter  $\frac{\sigma}{\sqrt{E_s \sigma_{cy}}}$ .

These dotted lines were established from the experimental crippling strength of the sandwiches determined from the tests at room temperature. The symbol shown on each of the room-temperature curves indicates an average value of the room-temperature experimental crippling strengths. The intersections of the dotted curves with the solid curves define the crippling stresses for the sandwiches at elevated temperatures.

## APPENDIX C

## BUCKLING STRENGTH OF SANDWICH COLUMNS

The maximum strength of the honeycomb-core sandwiches shown by the solid curves in figures 9(a) and 10(a) was determined from the following relation given in reference 5 which defines the buckling strength of a sandwich plate column and includes the effect of the shear modulus of the core on the buckling strength:

$$P_{cr(\text{elastic})} = \frac{1}{\frac{1}{P_e} + \frac{1}{AG_c}} \quad (C1)$$

where  $P_e$  is the Euler load for a plate column with clamped ends,  $A$  is an area equal to  $\frac{1}{2}(h + h_c)w$ , and  $G_c$  is the shear modulus of the core. The predicted load  $P_{cr(\text{elastic})}$  was reduced by a factor  $\eta$  when the predicted load exceeded the proportional limit stress for the material as follows:

$$P_{cr} = \eta P_{cr(\text{elastic})} \quad (C2)$$

where

$$\eta = \frac{E_t}{E} \quad (C3)$$

The magnitude of  $\eta$  was established from the compressive stress-strain curves for the face-sheet material given in figure 13.

The magnitude of  $G_c$  for use in equation (C1) was determined from the shear modulus tests made at room temperature on the cores described in the section entitled "Specimens, Equipment, and Procedures." The results of these tests on the square-cell and hexagonal-cell cores are shown in figure 15. The magnitude of  $G_c$  at elevated temperatures was calculated from the following relation:

$$G_c = G \frac{\rho_c}{\rho_f} C \quad (C4)$$

where  $G$  is the shear modulus of elasticity,  $\frac{\rho_c}{\rho_f}$  defines the solidity of the core, and  $C$  defines the fraction of the core material that is effective in resisting shear in the loading direction. The experimental values of  $C$  were 0.26 and 0.13, respectively, for the square-cell and hexagonal-cell cores. Theoretical values for  $C$  are, respectively, 0.5 and 0.375. The experimental values of  $C$  are less than the theoretical values and, therefore, suggest that the core elements of the sandwiches may have been buckled during fabrication or during machining of the test specimens.

## APPENDIX D

## EFFECTIVE STRESS-STRAIN CURVES

The analysis of structures fabricated from anisotropic materials is frequently based on the concept of effective stress-strain curves (see, for example, refs. 7 and 8). In this investigation the buckling and crippling stresses for the type 301 stainless-steel sandwiches were predicted with the aid of effective stress-strain curves derived from the material stress-strain curves given in figure 12. The effective stress-strain curves represent a weighted average of the longitudinal and transverse material properties for each temper. In this study the material stress-strain curves corresponding to the loading direction of the sandwich were weighted twice as heavily as the stress-strain curves transverse to the loading direction. The weighting procedure was accomplished by use of the following equation given in reference 9:

$$\epsilon = \frac{\sigma}{E} + 0.002 \left( \frac{\sigma}{\sigma_{cy}} \right)^n \quad (D1)$$

In this equation  $n$  is defined as the stress-strain curve shape parameter and is obtained from the equation

$$n = \frac{0.301}{\log_{10} \left( \frac{\sigma_{cy}}{\sigma_{0.001}} \right)} \quad (D2)$$

and  $\sigma_{0.001}$  defines the 0.1-percent-offset compressive-yield stress.

The values of  $n$  obtained from the stress-strain curves in figure 12 range from 4 to 8.

The effective stress-strain curves for the face sheets and for the cores were obtained by first determining the magnitude of the parameters  $E$ ,  $\sigma_{cy}$ , and  $n$  from each of the material stress-strain curves shown in figure 12. These parameters were then weighted twice as heavily in the loading direction of the sandwich as in the transverse direction. The weighted values of the parameters were then substituted into equation (D1) to calculate the effective stress-strain curves for each temper of the type 301 stainless steel.

## REFERENCES

1. Setterholm, V. C., and Kuenzi, E. W.: Performance of Stainless Steel Sandwich Construction at High Temperatures. WADC Tech. Rep. 55-417, ASTIA Doc. No. AD 97288, U. S. Air Force, Sept. 1956.
2. Anderson, Melvin S., and Updegraff, Richard G.: Some Research Results on Sandwich Structures. NACA TN 4009, 1957.
3. Stein, Bland A.: Compressive Stress-Strain Properties of 17-7 PH and AM 350 Stainless-Steel Sheet at Elevated Temperatures. NACA TN 4074, 1957.
4. Anderson, Melvin S.: Local Instability of the Elements of a Truss-Core Sandwich Plate. NACA TN 4292, 1958.
5. Boller, K. H., and Norris, C. B.: Effect of Shear Strength on Maximum Loads of Sandwich Columns. Rep. No. 1815 (Contract Nos. NBA-PO-NAer 00845 and USAF-PO-(33-038)49-4696E), Forest Products Lab., U. S. Dept. Agriculture, June 1950.
6. Stowell, Elbridge Z.: A Unified Theory of Plastic Buckling of Columns and Plates. NACA Rep. 898, 1948. (Supersedes NACA TN 1556.)
7. Anderson, Roger A., and Anderson, Melvin S.: Correlation of Crippling Strength of Plate Structures With Material Properties. NACA TN 3600, 1956.
8. Watter, Michael, and Lincoln, Rush A.: Strength of Stainless Steel Structural Members as Function of Design. First ed., Allegheny Ludlum Steel Corp. (Pittsburgh), 1950.
9. Hill, H. N.: Determination of Stress-Strain Relations From "Offset" Yield Strength Values. NACA TN 927, 1944.

TABLE I

## COMPRESSIVE-STRENGTH TEST RESULTS FOR SANDWICH SPECIMENS

[All specimens exposed to test temperature for 30 minutes prior to loading;  
nominal rate of unit shortening, 0.005 per minute]

## (a) Corrugated-core sandwich specimens

17-7 PH stainless-steel specimens with single-corrugated cores							
Equal-thickness face sheets				Unequal-thickness face sheets			
Specimen number	Test temperature, °F	$\bar{\sigma}_f$ , ksi	$\bar{\epsilon}_f$	Specimen number	Test temperature, °F	$\bar{\sigma}_f$ , ksi	$\bar{\epsilon}_f$
1	80	154	0.0057	14	90	164	0.0067
2	80	147	.0060	15	80	165	.0075
3	80	144	.0064	16	80	166	.0086
4	208	152	.0063	17	213	157	.0067
5	393	138	.0062	18	396	145	.0062
6	404	125	*	19	602	134	0.0070
7	400	120	0.0056	20	802	128	.0071
8	597	133	.0060	21	892	113	.0065
9	799	111	.0048	22	997	76	.0065
10	902	113	.0064	23	1100	44	.0079
11	996	82	0.0080	24	1198	31	0.0073
12	1099	46	.0090				
13	1195	34	.0120				
Type 301 stainless-steel specimens with double-corrugated cores							
Specimen weight, 1 lb/sq ft				Specimen weight, 2 lb/sq ft			
Specimen number	Test temperature, °F	$\bar{\sigma}_f$ , ksi	$\bar{\epsilon}_f$	Specimen number	Test temperature, °F	$\bar{\sigma}_f$ , ksi	$\bar{\epsilon}_f$
25	90	136	0.0073	37	80	176	0.0079
26	80	142	.0097	38	80	178	.0075
27	80	134	.0068	39	80	164	.0063
28	208	128	.0067	40	204	160	.0071
29	406	120	.0080	41	207	145	.0071
30	600	110	0.0068	42	403	156	0.0078
31	712	119	.0075	43	590	152	.0074
32	800	113	.0065	44	597	128	.0064
33	901	98	.0070	45	798	126	.0073
34	1007	74	.0080	46	905	126	.0096
35	1099	58	*	47	1003	84	0.0096
36	1198	54	0.0098	48	1100	69	.0122
				49	1198	52	.0125

\*Magnitude of  $\bar{\epsilon}_f$  not determined because of malfunction of strain extensometer equipment.

TABLE I.- Concluded

## COMPRESSIVE-STRENGTH TEST RESULTS FOR SANDWICH SPECIMENS

## (b) Honeycomb-core sandwich specimens

Specimens with 17-7 PH stainless-steel face sheets and type 321 stainless-steel square-cell cores				Specimens with 17-7 PH stainless-steel face sheets and 17-7 PH stainless-steel hexagonal-cell cores			
Specimen number	Test temperature, $^{\circ}\text{F}$	$\bar{\sigma}_f$ , ksi	$\bar{\epsilon}_f$	Specimen number	Test temperature, $^{\circ}\text{F}$	$\bar{\sigma}_f$ , ksi	$\bar{\epsilon}_f$
50	80	160	0.0071	71	80	144	0.0052
51	78	160	.0064	72	80	135	.0068
52	80	142	.0088	73	80	143	*
53	80	108	.0039	74	201	138	.0050
54	200	82	.0036	75	401	98	.0042
55	201	107	0.0045	76	410	112	0.0047
56	200	113	.0043	77	498	128	.0054
57	206	108	.0049	78	595	114	.0046
58	408	132	.0034	79	698	136	.0062
59	400	111	.0044	80	800	137	.0058
60	503	143	0.0057	81	900	126	0.0056
61	510	104	.0043	82	1002	86	.0095
62	501	82	.0032	83	1099	50	.0100
63	503	124	.0050	84	1198	36	.0140
64	600	124	.0051				
65	699	108	0.0043				
66	800	87	.0038				
67	902	90	.0045				
68	1004	71	.0049				
69	1095	63	.0212				
70	1194	40	.0440				

\*Magnitude of  $\bar{\epsilon}_f$  not determined because of malfunction of strain extensometer equipment.

TABLE II

## COMPRESSIVE STRESS-STRAIN PROPERTIES FOR EXTRA-HARD AND

## FULL-HARD TEMPER TYPE 301 STAINLESS STEEL\*

[Specimen size, 2.70 in. long, 0.65 in. wide, 1.5 in. gage length;  
loading rate, 0.02 in./in./min head speed; exposure time at test  
temperature prior to loading, 10 to 20 minutes]

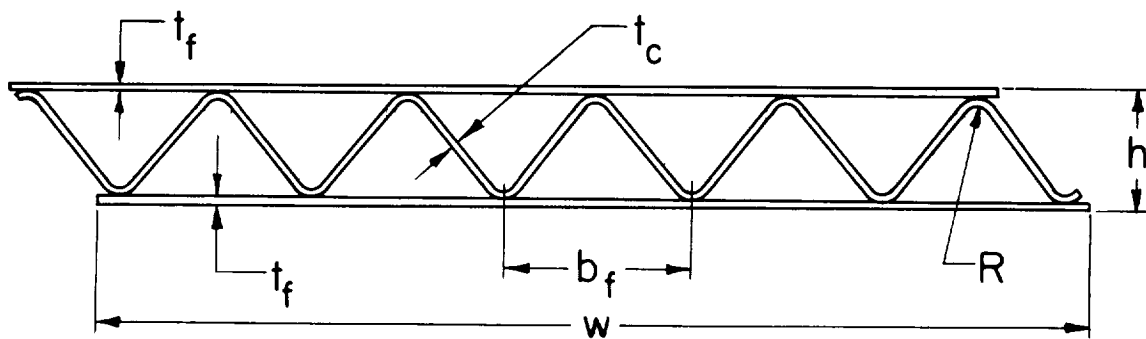
Temper: Extra hard Heat no.: 334967 Sheet thickness: 0.027 in. Cold rolled 65 percent, stress relieved for 8 hr at 750° F Rockwell hardness: RC 52.0 Chemical composition, percent by weight: Carbon, 0.11; Manganese, 0.57; Silicon, 0.50; Chromium, 17.25; Nickel, 7.00				
Test temperature, °F	Longitudinal properties		Transverse properties	
	$\sigma_{cy}$ , ksi	E, ksi	$\sigma_{cy}$ , ksi	E, ksi
70	235.5	$27.5 \times 10^3$	323.4	$31.8 \times 10^3$
400	204.2	26.0	285.5	29.4
600	173.3	23.4	257.9	27.7
800	146.3	21.2	232.2	24.6
900	139.5	20.1	192.3	22.1
1000	86.8	16.6	117.0	18.1

Temper: Full hard Heat no.: 326332 Sheet thickness: 0.032 in. Cold rolled 40 percent, stress relieved for 8 hr at 800° F Rockwell hardness: RC 46.0 Chemical composition, percent by weight: Carbon, 0.12; Manganese, 0.76; Silicon, 0.43; Chromium, 17.07; Nickel, 7.23				
Test temperature, °F	Longitudinal properties		Transverse properties	
	$\sigma_{cy}$ , ksi	E, ksi	$\sigma_{cy}$ , ksi	E, ksi
70	165.0	$26.4 \times 10^3$	214.0	$28.3 \times 10^3$
400	134.5	26.0	199.0	26.7
600	124.3	24.7	191.0	25.5
800	105.0	22.1	166.8	21.6
900	97.0	21.0	156.9	20.2
1000	83.7	20.3	137.1	20.3

\*These data furnished by Allegheny Ludlum Steel Corporation, Research and Development Laboratories, Brackenridge, Pennsylvania.





Material: 17-7 PH stainless steel.

Fabricator: The Budd Company, Philadelphia, Pennsylvania.

$w = 2.20$  in.

$L = 2.50$  in.

$h = 0.24$  in.

$b_f = 0.394$  in.

$t_f = 0.0156$  in.

$t_c = 0.0125$  in.

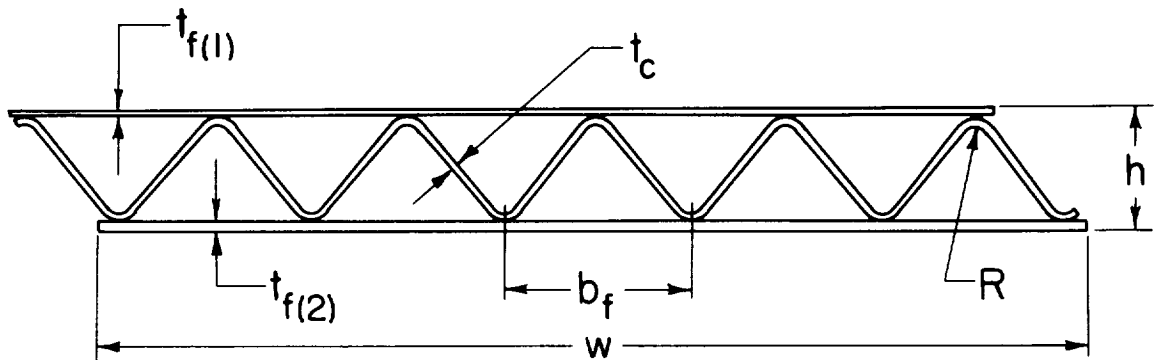
$R = 0.05$  in.

Weight = 2 lb/sq ft

Compressive load applied in direction of corrugations.

(a) Cross section of resistance-welded single-corrugated-core sandwich with equal-thickness face sheets.

Figure 1.- Sandwich-specimen information. All indicated dimensions are nominal values.



Material: 17-7 PH stainless steel.

Fabricator: The Budd Company, Philadelphia, Pennsylvania.

$$w = 2.20 \text{ in.}$$

$$L = 2.50 \text{ in.}$$

$$h = 0.24 \text{ in.}$$

$$b_f = 0.394 \text{ in.}$$

$$t_{f(1)} = 0.0125 \text{ in.}$$

$$t_{f(2)} = 0.0188 \text{ in.}$$

$$t_c = 0.0125 \text{ in.}$$

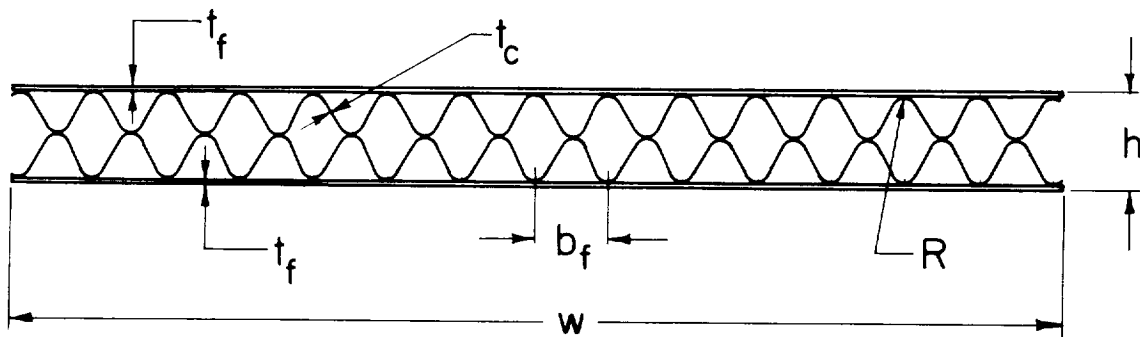
$$R = 0.05 \text{ in.}$$

$$\text{Weight} = 2 \text{ lb/sq ft}$$

Compressive load applied in direction of corrugations.

(b) Cross section of resistance-welded single-corrugated-core sandwich with unequal-thickness face sheets.

Figure 1.- Continued.



Material: Stress-relieved type 301 stainless steel; face sheets, extra-hard temper with longitudinal grain direction in direction of corrugations; corrugations, full-hard temper with longitudinal grain direction in direction of corrugations.

Fabricator: The Budd Company, Philadelphia, Pennsylvania.

$$w = 2.25 \text{ in.}$$

$$L = 2.00 \text{ in.}$$

$$h = 0.20 \text{ in.}$$

$$b_f = 0.160 \text{ in.}$$

$$t_f = 0.005 \text{ in.}$$

$$t_c = 0.0044 \text{ in.}$$

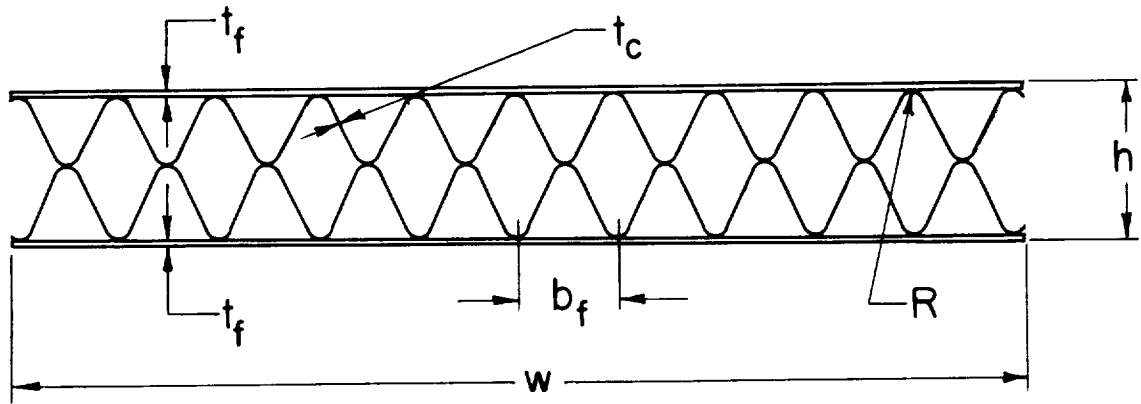
$$R = 1/32 \text{ in.}$$

$$\text{Weight} = 1 \text{ lb/sq ft}$$

Compressive load applied in direction of corrugations.

(c) Cross section of resistance-welded double-corrugated-core sandwich.

Figure 1.- Continued.



Material: Stress-relieved type 301 stainless steel; face sheets, extra-hard temper with longitudinal grain direction in direction of corrugations; corrugations, full-hard temper with transverse grain direction in direction of corrugations.

Fabricator: The Budd Company, Philadelphia, Pennsylvania.

$$w = 2.20 \text{ in.}$$

$$L = 2.50 \text{ in.}$$

$$h = 0.314 \text{ in.}$$

$$b_f = 0.212 \text{ in.}$$

$$t_f = 0.014 \text{ in.}$$

$$t_c = 0.006 \text{ in.}$$

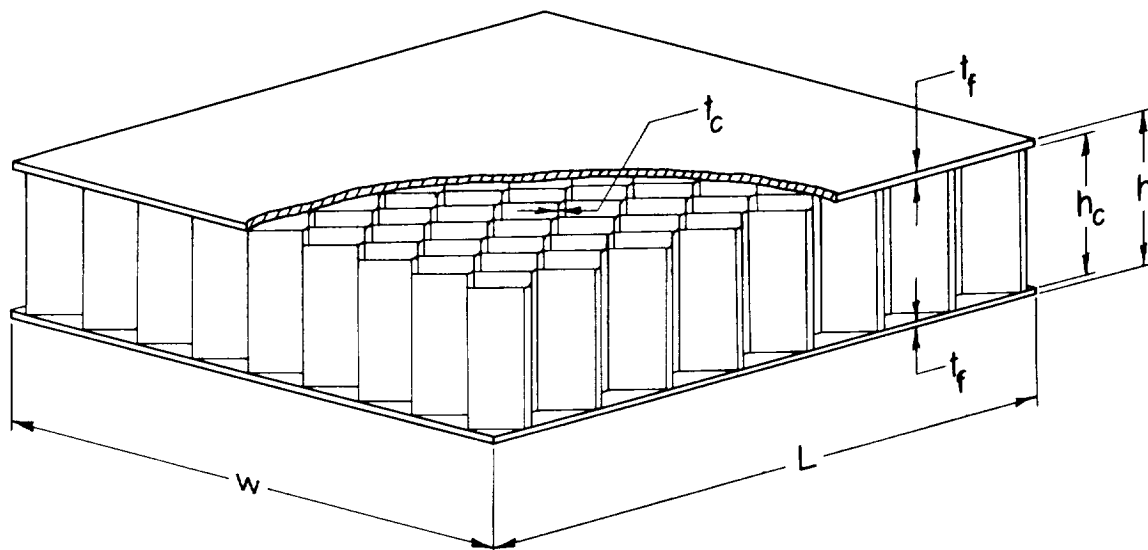
$$R = 1/32 \text{ in.}$$

$$\text{Weight} = 2 \text{ lb/sq ft}$$

Compressive load applied in direction of corrugations.

(d) Cross section of resistance-welded double-corrugated-core sandwich.

Figure 1.- Continued.



Material: 17-7 PH stainless-steel face sheets; type 321 stainless-steel core.

Fabricator: The Martin Company, Baltimore, Maryland.

$w = 2.20$  in.

$L = 2.50$  in.

$h = 0.70$  in.

$h_c = 0.625$  in.

$t_f = 0.032$  in.

$t_c = 0.002$  in.

Weight = 3.4 lb/sq ft

Cell size =  $1/4$  in.

Core density = 7.7 lb/cu ft

Brazed in muffle furnace in helium atmosphere.

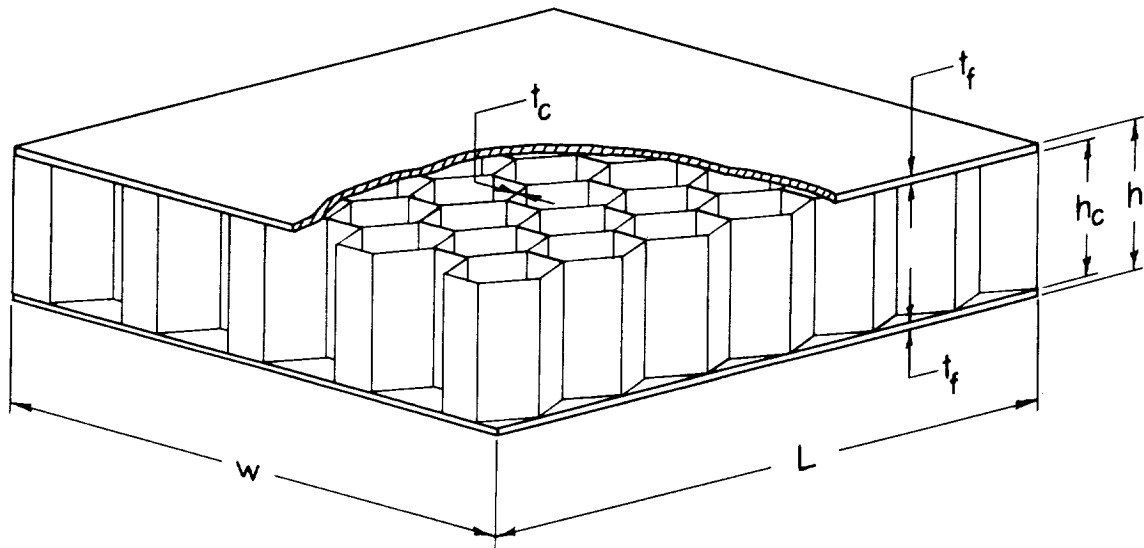
Brazing alloy: Coast metal No. 53, 0.26 lb/sq ft of sandwich.

Heat treated at  $1,125^{\circ}$  F after brazing.

Compressive load applied in direction of core ribbons.

(e) Brazed honeycomb-core sandwich with square-cell cores.

Figure 1.- Continued.



Material: 17-7 PH stainless-steel faces and core.

Fabricator: The Martin Company, Baltimore, Maryland.

$w = 2.20$  in.

$L = 2.50$  in.

$h = 0.70$  in.

$h_c = 0.625$  in.

$t_f = 0.032$  in.

$t_c = 0.0015$  in.

Weight = 3.1 lb/sq ft

Cell size =  $3/8$  in. (distance across flats)

Core density = 5.1 lb/cu ft

Brazed in muffle furnace in helium atmosphere.

Brazing alloy: Coast metal No. 53, 0.26 lb/sq ft of sandwich.

Heat treated at  $1,125^{\circ}$  F after brazing.

Compressive load applied perpendicular to direction of core ribbons.

(f) Brazed honeycomb-core sandwich with hexagonal-cell cores.

Figure 1.- Concluded.

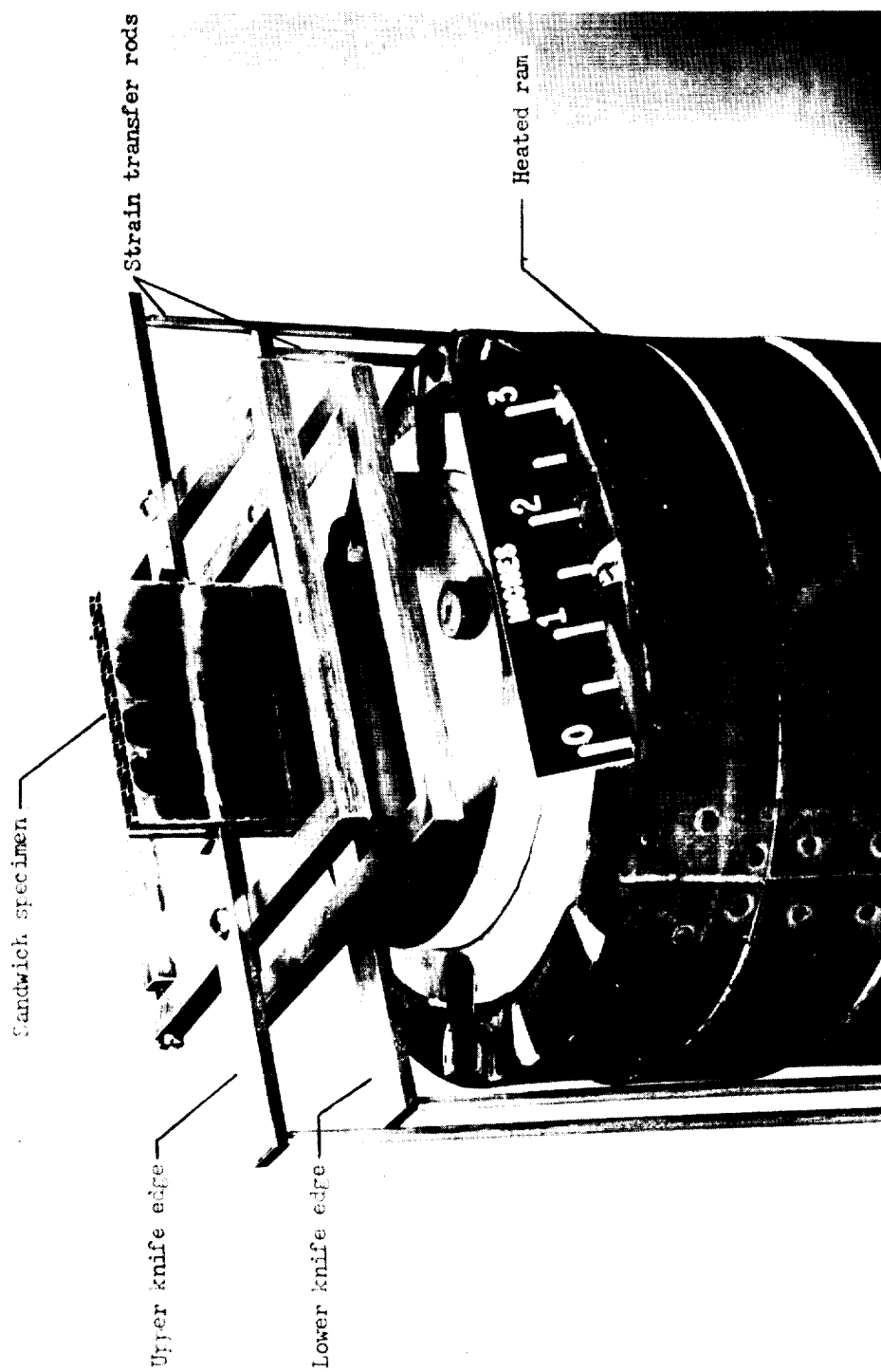
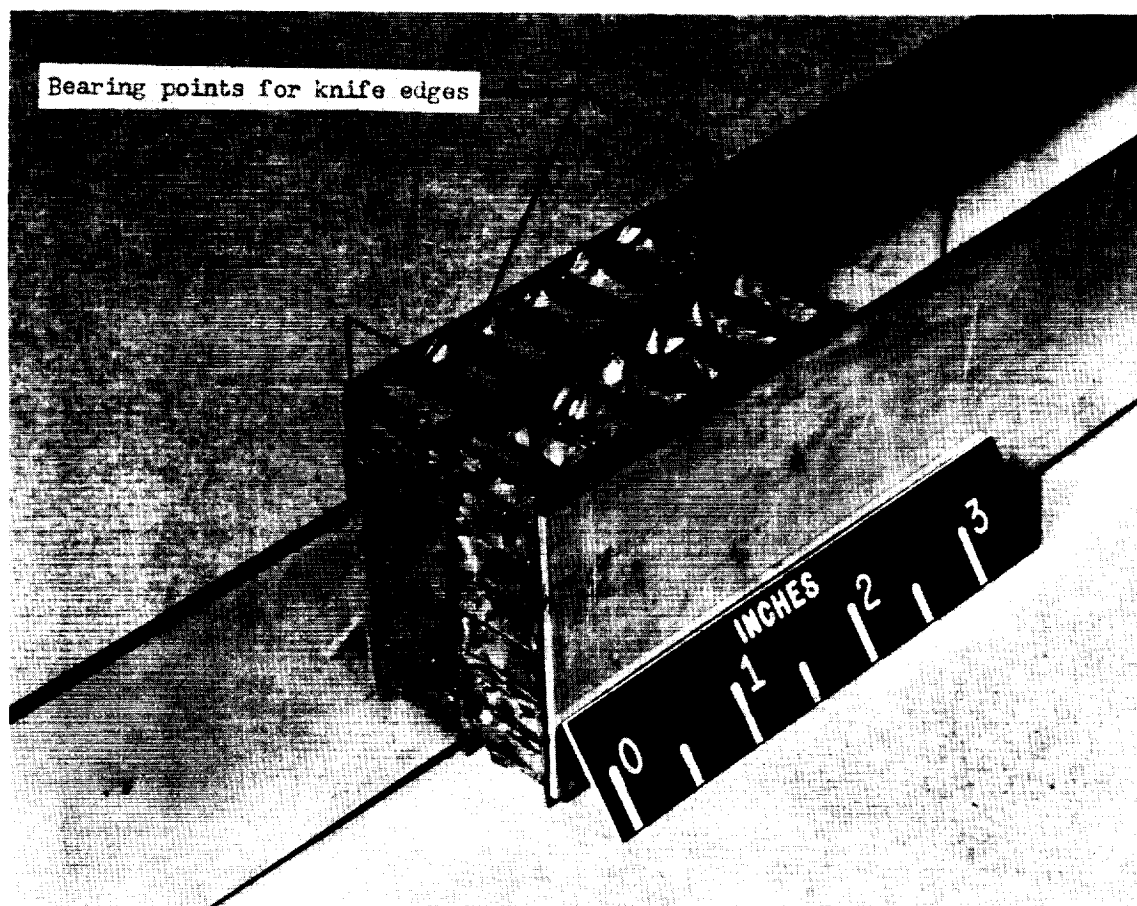
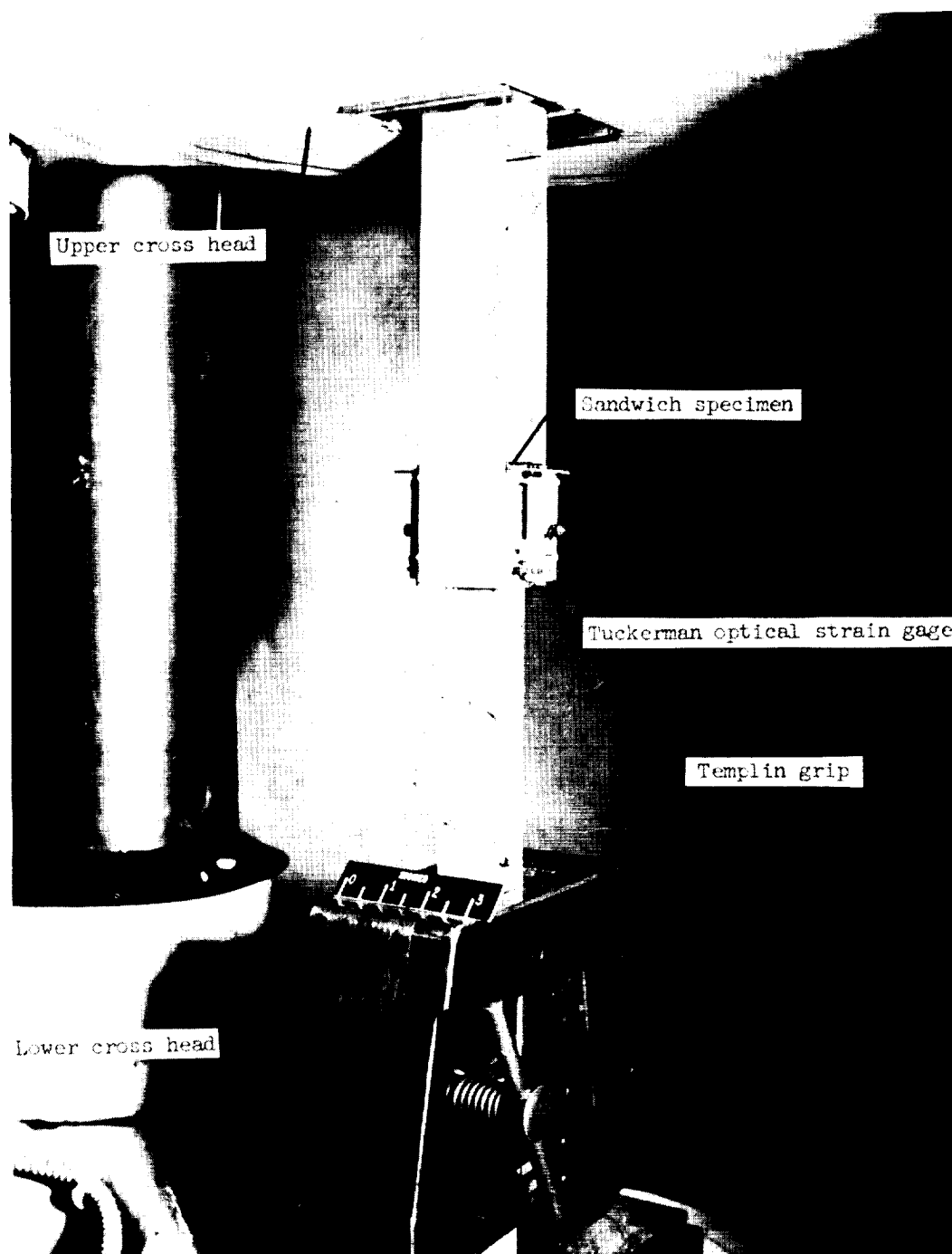


Figure 2.- Extensometer assembly used for determination of unit shortening of sandwich specimens.

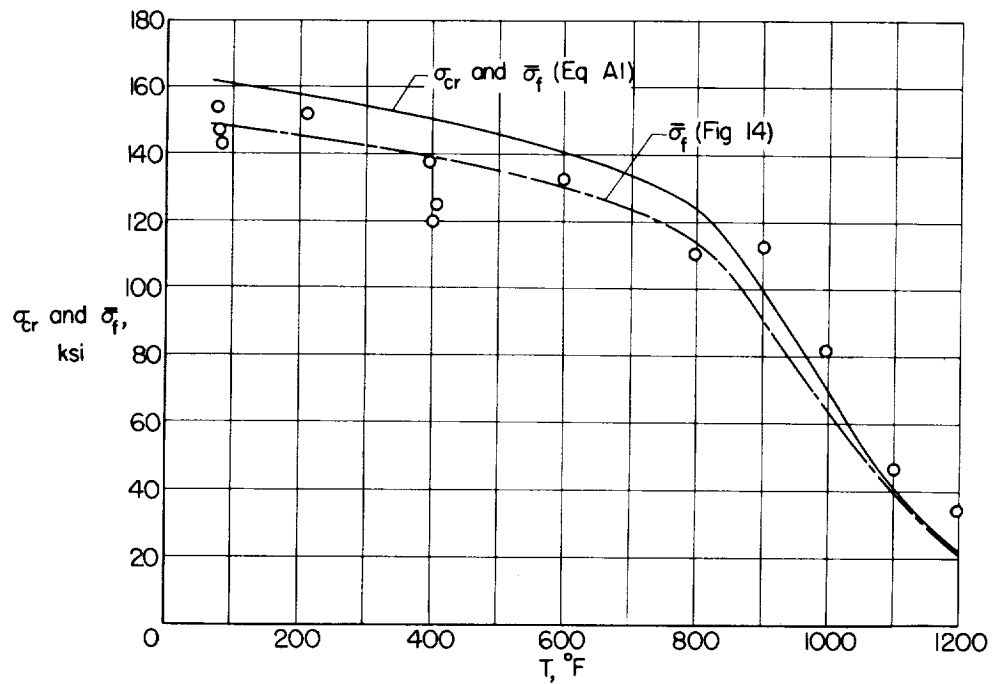


L-58-1763.1  
Figure 3.- Assembly of sandwich specimens used for determination of shear modulus of honeycomb core at room temperature.

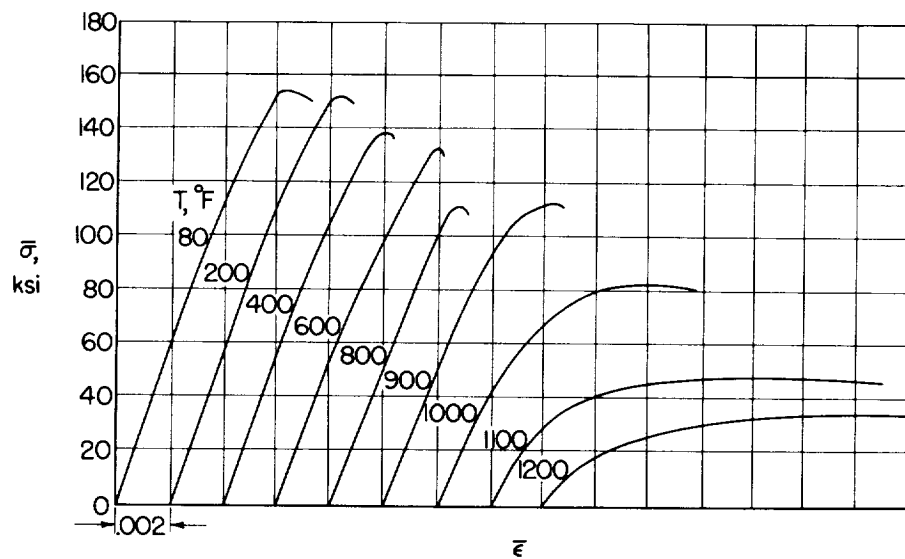




L-58-1762.1  
Figure 4.- Test setup for determination of shear modulus of honeycomb core.

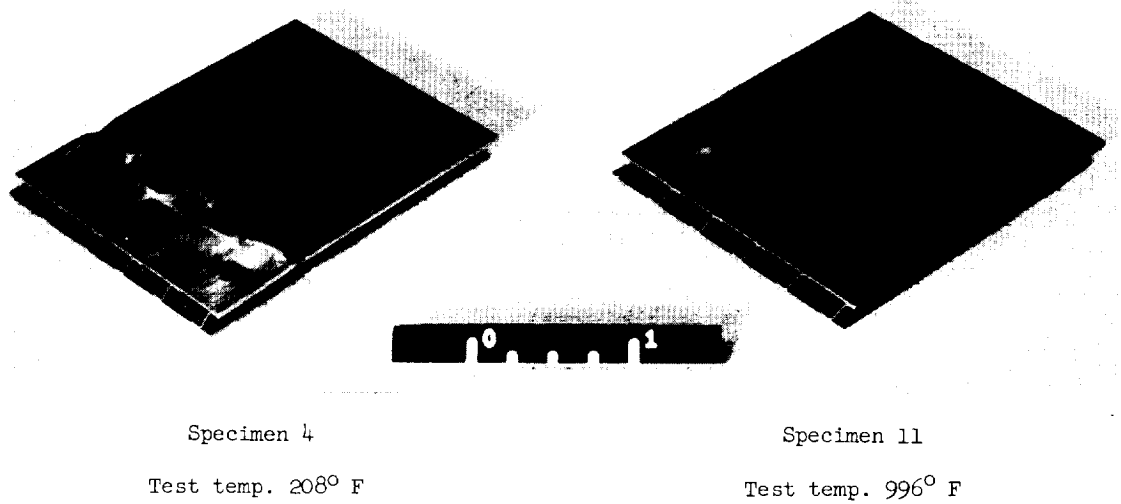


(a) Comparison between experimental maximum (cripling) stresses and predicted buckling and maximum (cripling) stresses.



(b) Experimental curves of average stress against unit shortening.

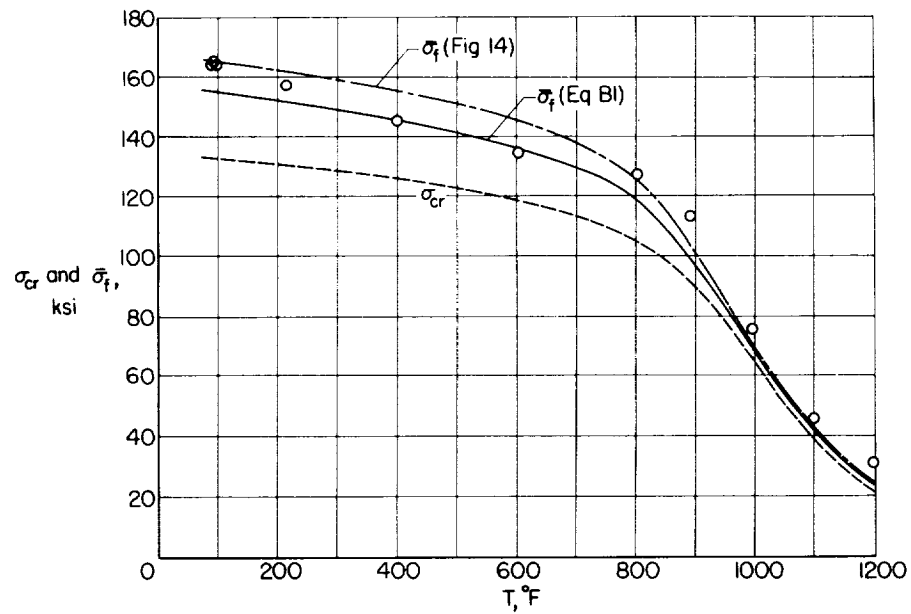
Figure 5.- Test results for resistance-welded 17-7 PH stainless-steel single-corrugated-core sandwiches with equal-thickness face sheets.



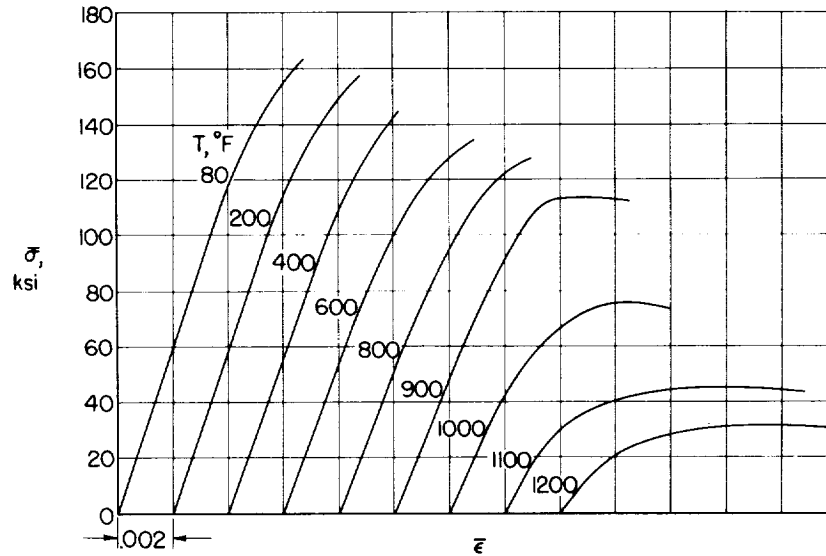
L-58-1128.1

(c) View of tested specimens showing buckle pattern and mode of failure.

Figure 5.- Concluded.

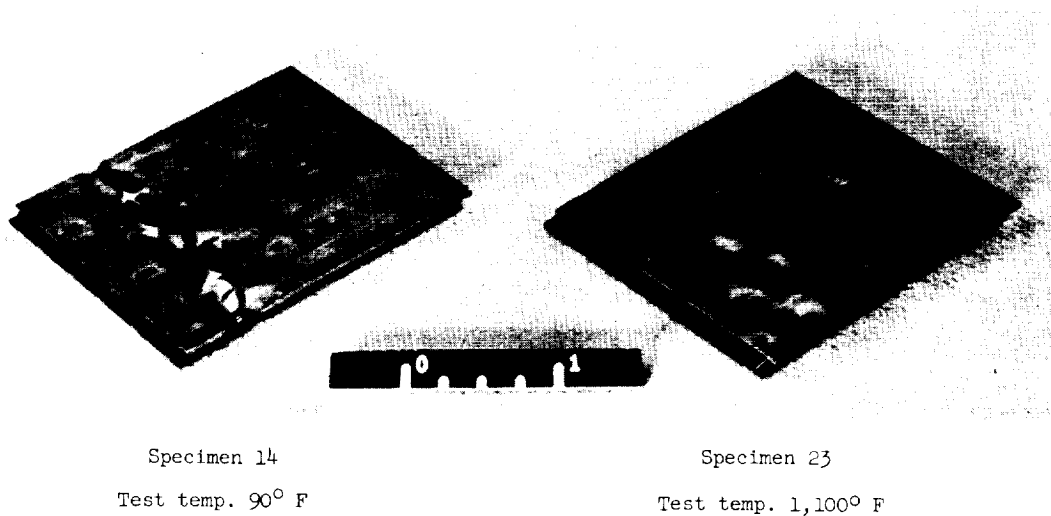


(a) Comparison between experimental maximum (crippling) stresses and predicted buckling and maximum (crippling) stresses.



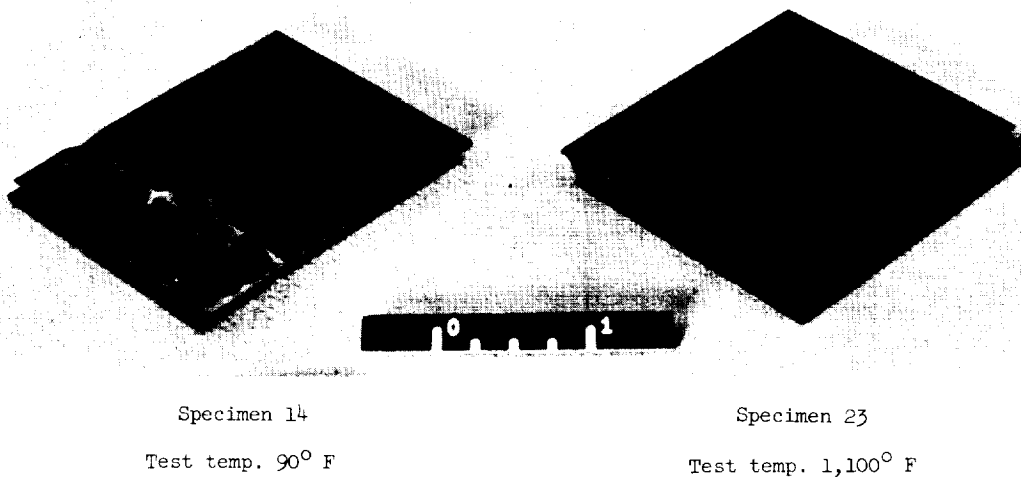
(b) Experimental curves of average stress against unit shortening.

Figure 6.- Test results for resistance-welded 17-7 PH stainless-steel single-corrugated-core sandwiches with unequal-thickness face sheets.



L-58-1131.1

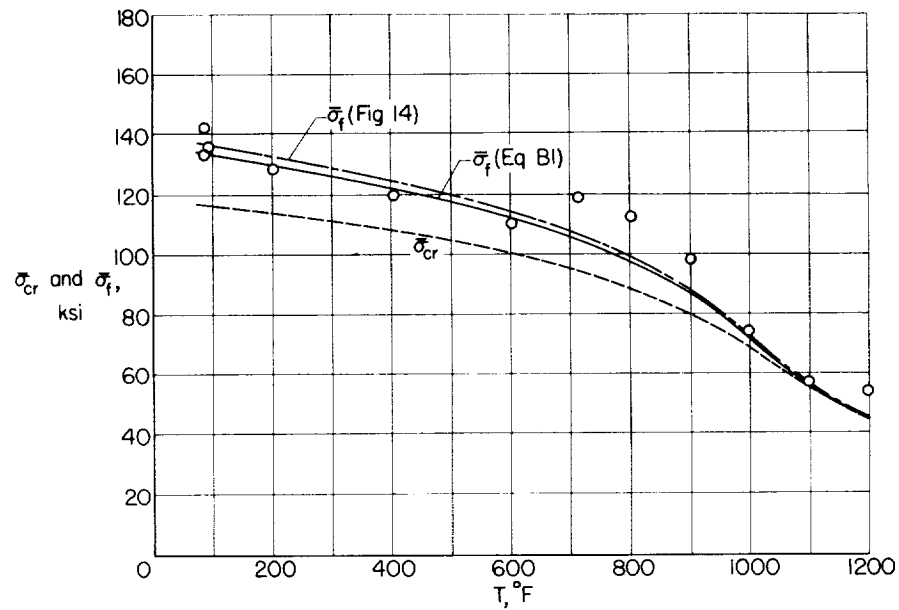
(c) View of tested specimens showing buckle pattern and mode of failure in thinner face sheet.



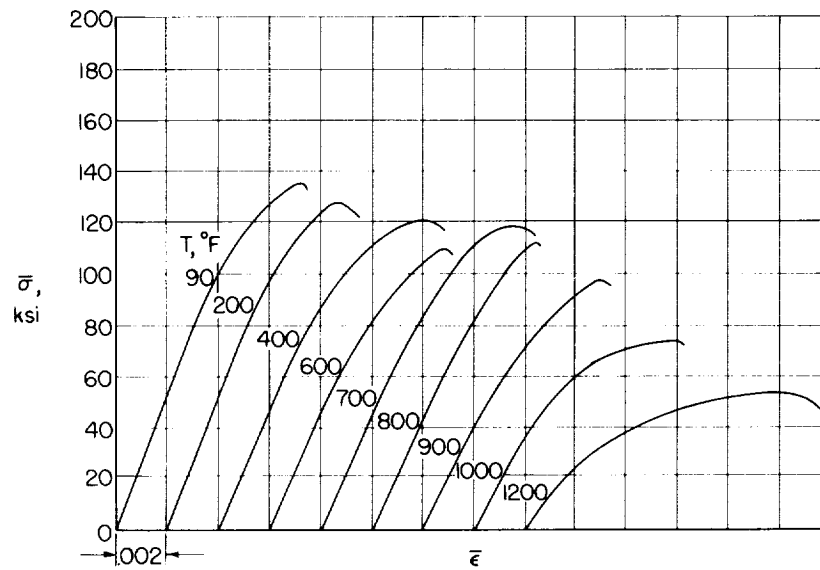
L-58-1132.1

(d) View of tested specimens showing buckle pattern and mode of failure in thicker face sheet.

Figure 6.- Concluded.

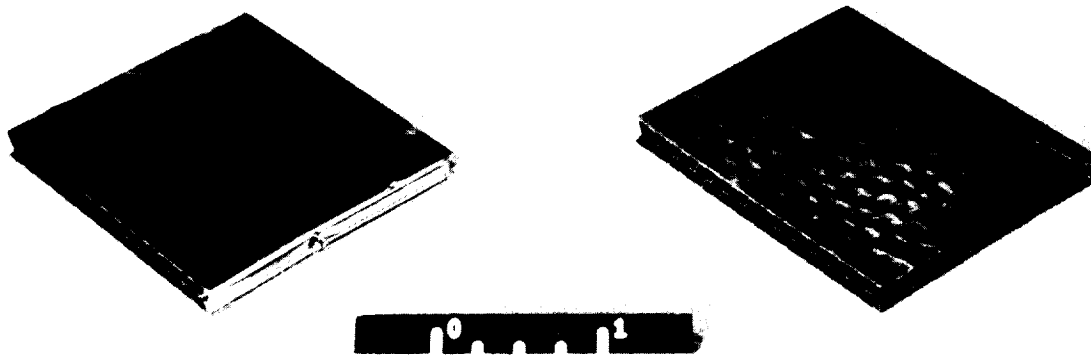


(a) Comparison between experimental maximum (crippling) stresses and predicted buckling and maximum (crippling) stresses.



(b) Experimental curves of average stress against unit shortening.

Figure 7.- Test results for resistance-welded type 301 stainless-steel double-corrugated-core sandwiches weighing 1 pound per square foot.



Specimen 28

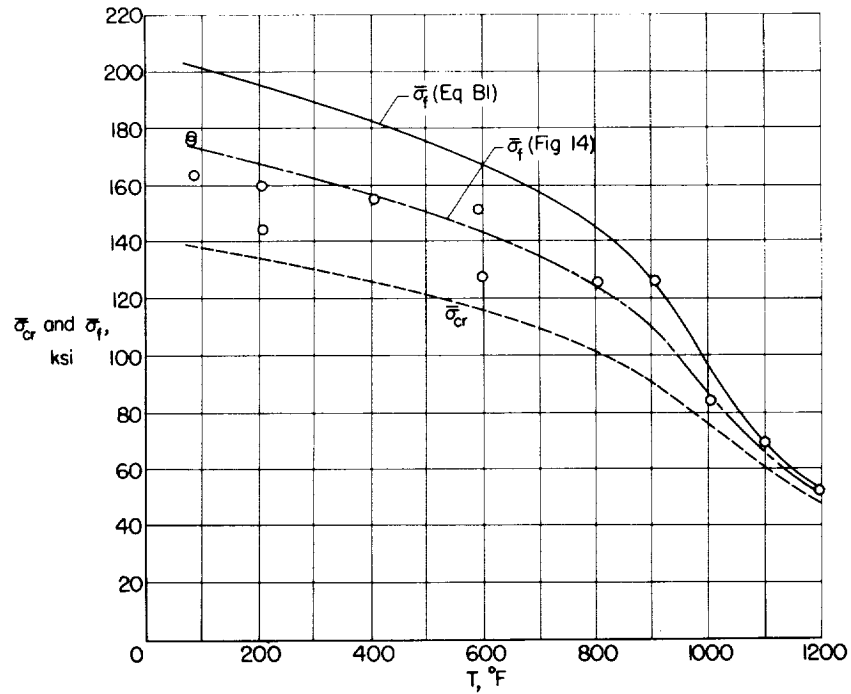
Test temp. 208° F

Specimen 34

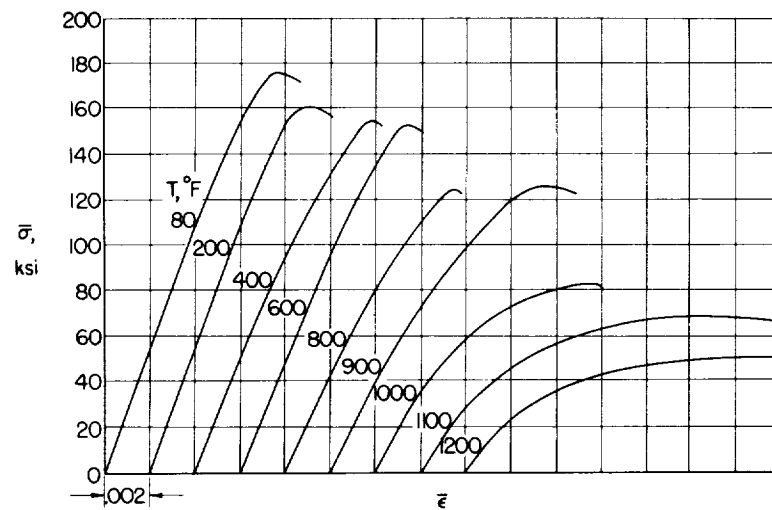
Test temp. 1,007° F

(c) View of tested specimen showing buckle pattern and mode of failure. L-58-1129.1

Figure 7.- Concluded.



(a) Comparison between experimental maximum (crippling) stresses and predicted buckling and maximum (crippling) stresses.



(b) Experimental curves of average stress against unit shortening.

Figure 8.- Test results for resistance-welded type 301 stainless-steel double-corrugated-core sandwiches weighing 2 pounds per square foot.





Specimen 37

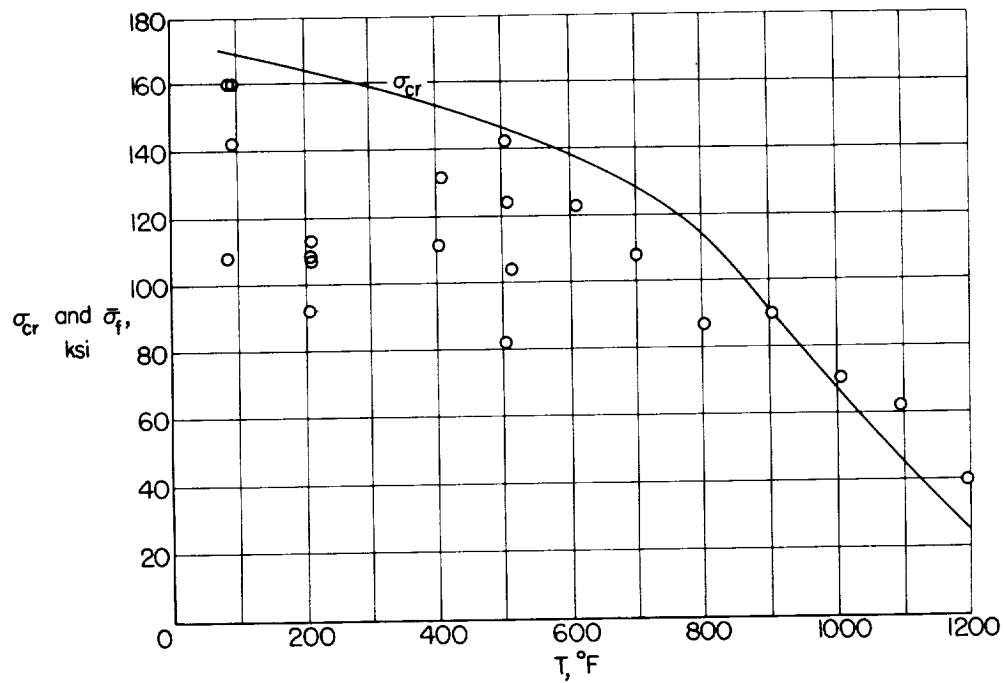
Test temp. 80° F

Specimen 49

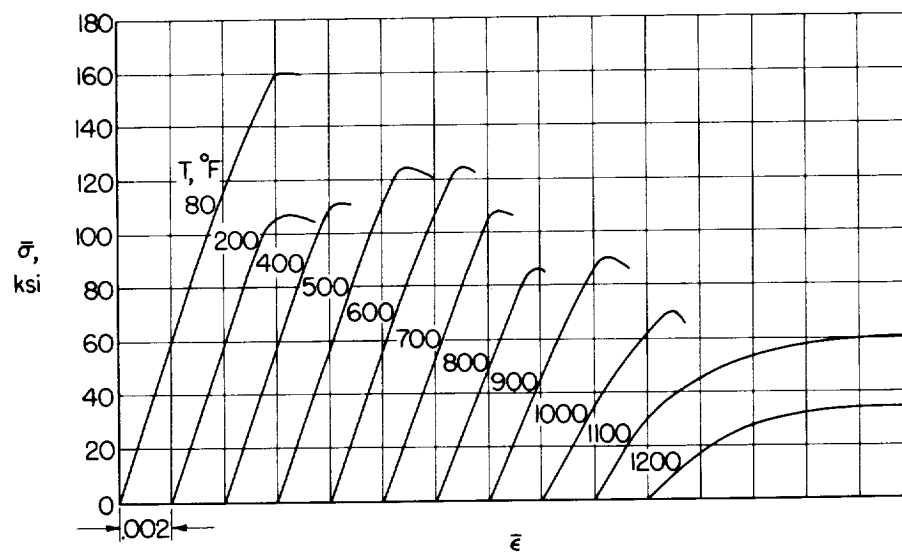
Test temp. 1,198° F

(c) View of tested specimen showing buckle pattern and mode of failure. L-58-1133.1

Figure 8.- Concluded.

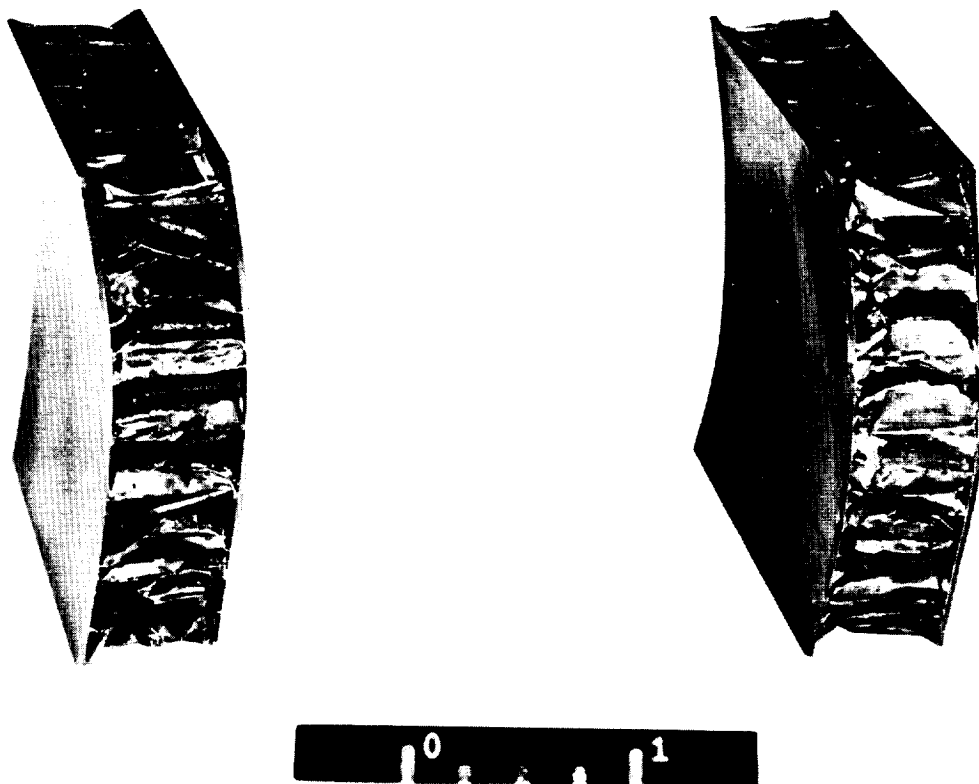


(a) Comparison between experimental maximum stresses and predicted buckling stresses.



(b) Experimental curves of average stress against unit shortening.

Figure 9.- Test results for brazed square-cell honeycomb-core sandwiches with 17-7 PH stainless-steel face sheets and type 321 stainless-steel cores.



Specimen 53

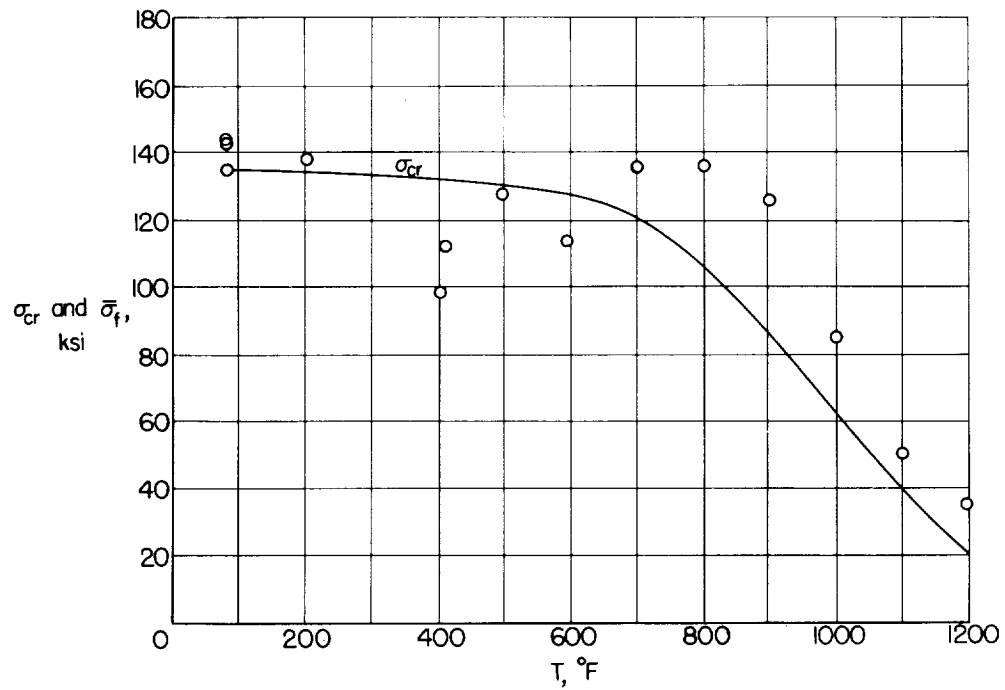
Test temp. 80° F

Specimen 68

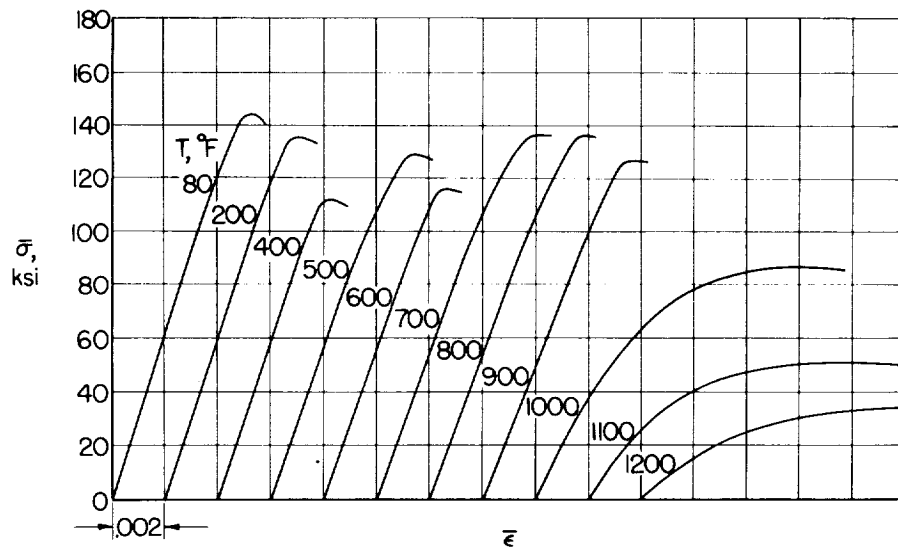
Test temp. 1,004° F

(c) View of tested specimens showing mode of failure. L-58-2880.1

Figure 9.- Concluded.

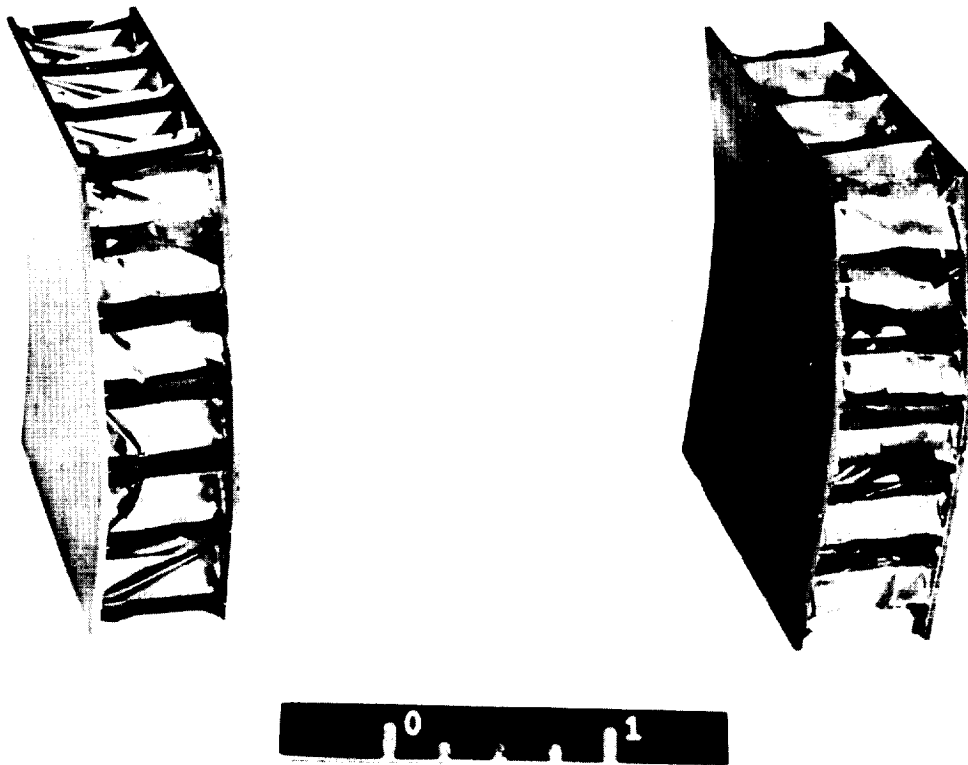


(a) Comparison between experimental maximum stresses and predicted buckling stresses.



(b) Experimental curves of average stress against unit shortening.

Figure 10.- Test results for brazed hexagonal-cell honeycomb-core sandwiches with 17-7 PH stainless-steel face sheets and cores.



Specimen 74

Test temp. 201° F

Specimen 82

Test temp. 1,002° F

L-58-2881.1

(c) View of tested specimens showing mode of failure.

Figure 10.- Concluded.

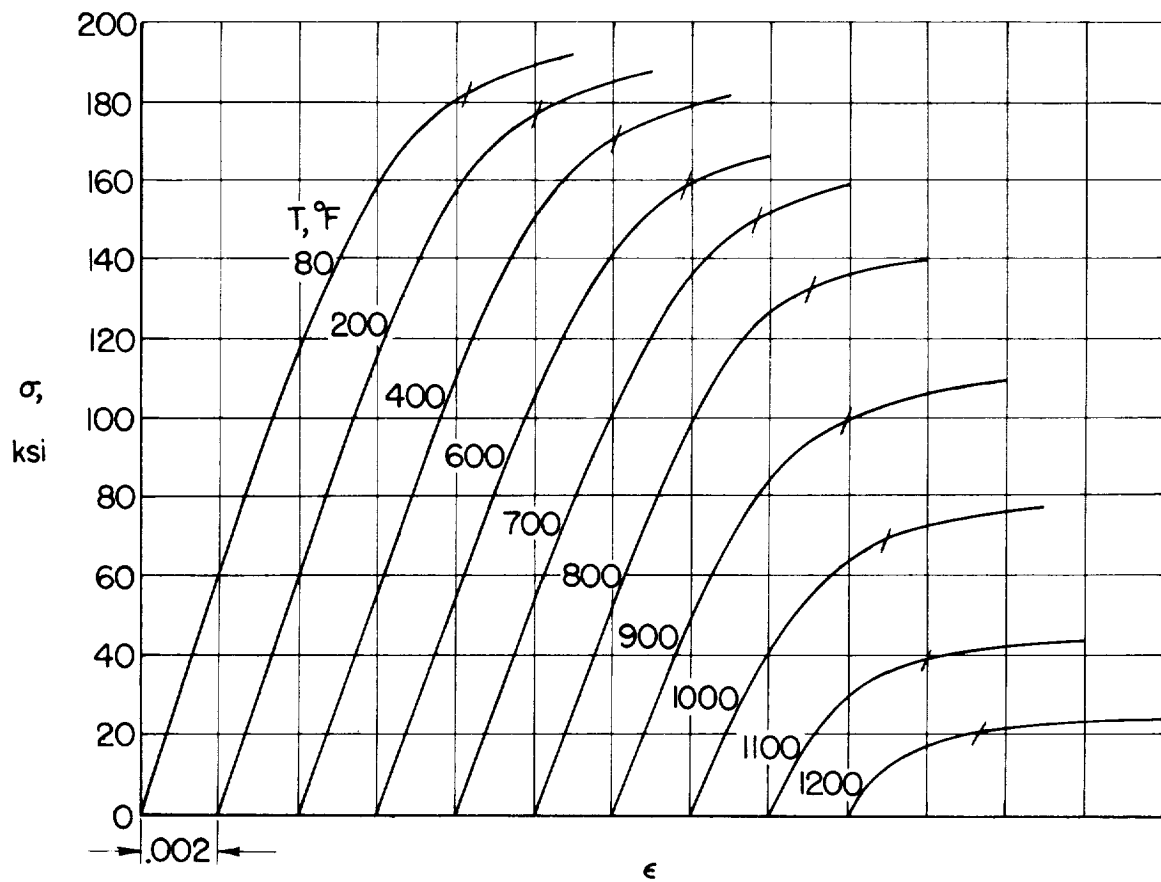
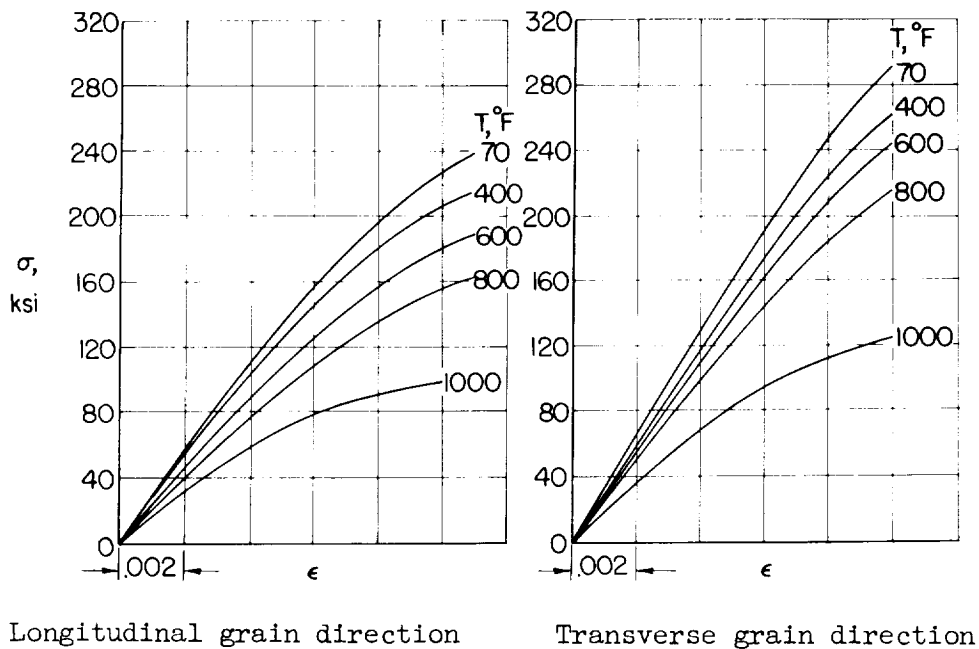
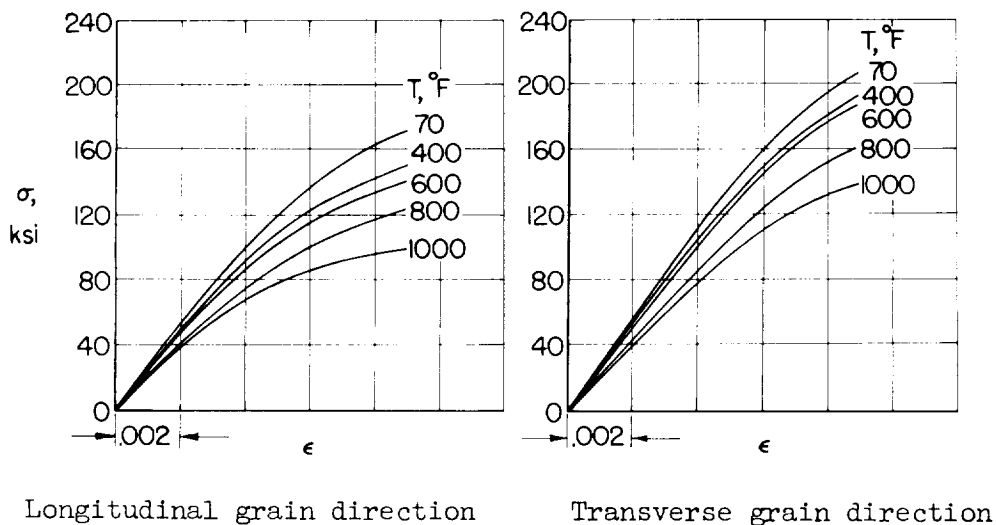


Figure 11.- Compressive stress-strain curves for 17-7 PH stainless-steel sheet, Condition TH 1050. Strain rate, 0.002 per minute; 1/2-hour exposure to test temperature. (Data from ref. 3.)

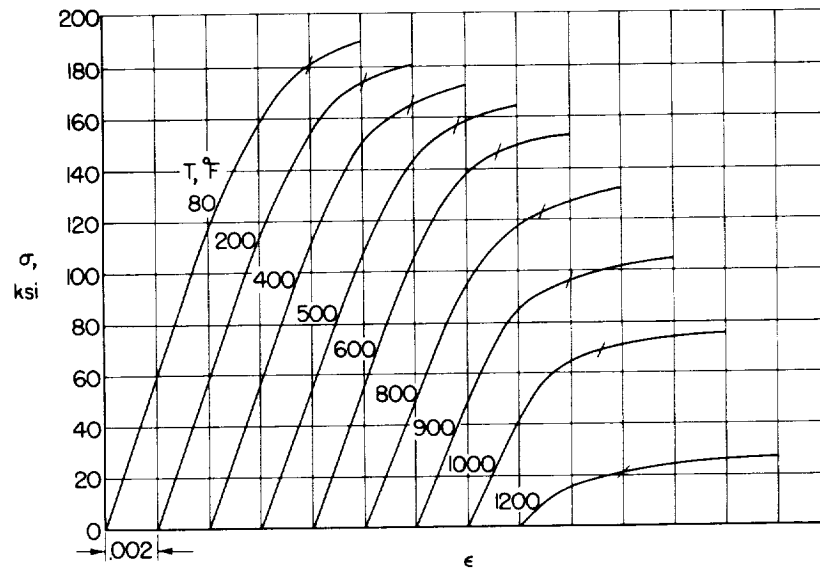


(a) Extra-hard temper; heat no. 334967.

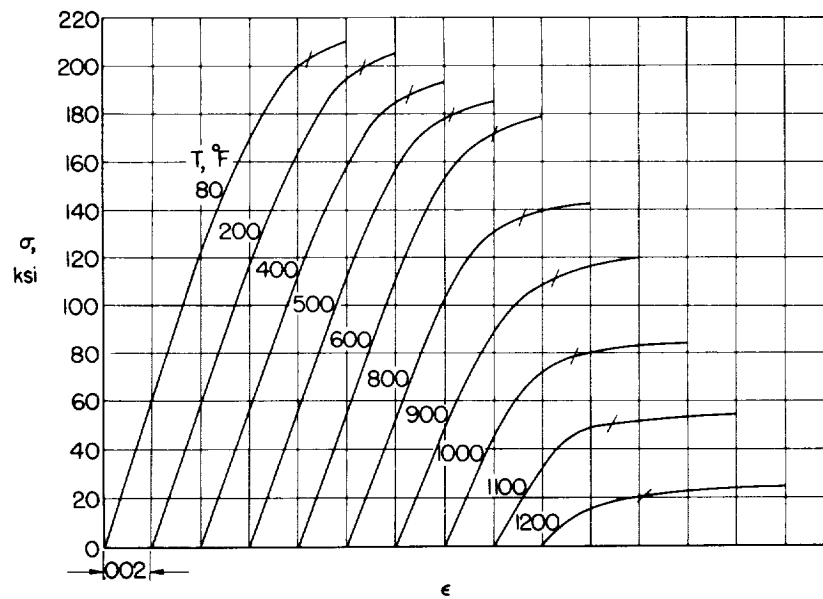


(b) Full-hard temper; heat no. 326332.

Figure 12.- Compressive stress-strain curves for stress-relieved type 301 stainless-steel sheet. Data furnished by Allegheny Ludlum Steel Corporation, Research and Development Laboratories, Brackenridge, Pennsylvania. See table II for properties of this material.



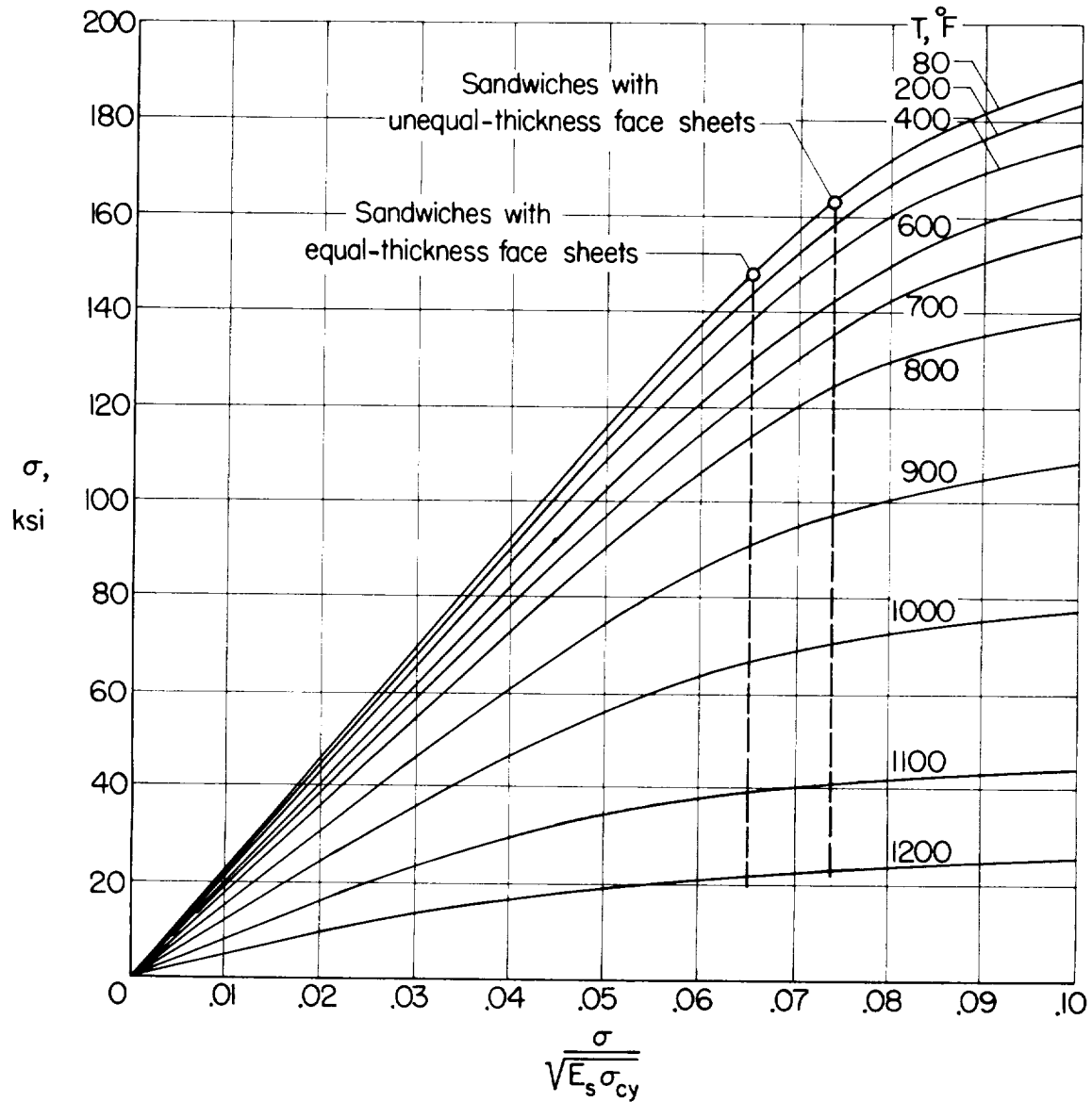
(a) Compressive stress-strain curves for face-sheet material from sandwiches having square-cell cores.



(b) Compressive stress-strain curves for face-sheet material from sandwiches having hexagonal-cell cores.

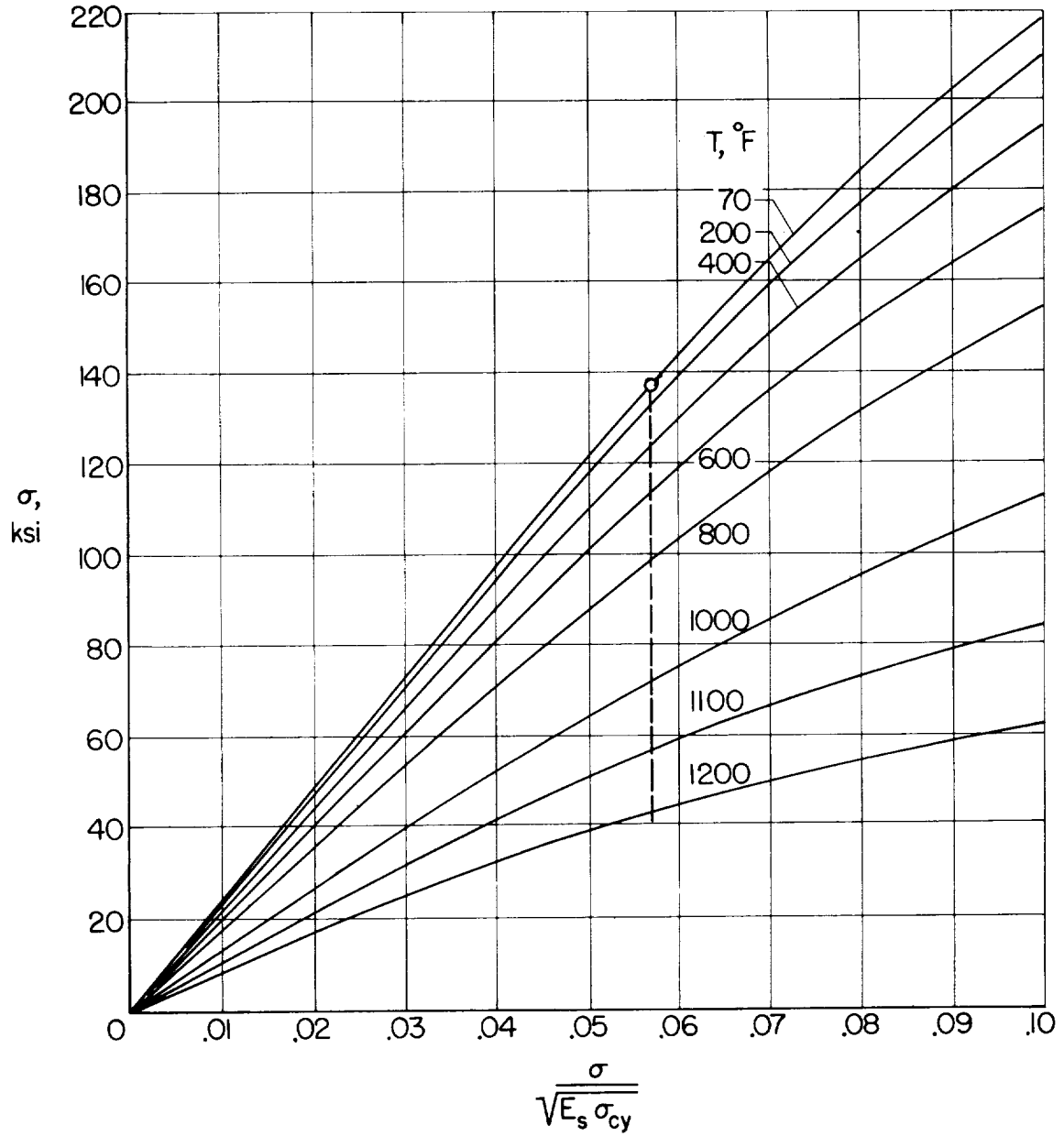
Figure 13.- Compressive stress-strain curves for 17-7 PH stainless-steel face-sheet material obtained from brazed honeycomb-core sandwiches. Sandwiches were heat treated at  $1,125^{\circ}\text{F}$  after brazing. Strain rate, 0.005 per minute; 1/2-hour exposure to test temperature.





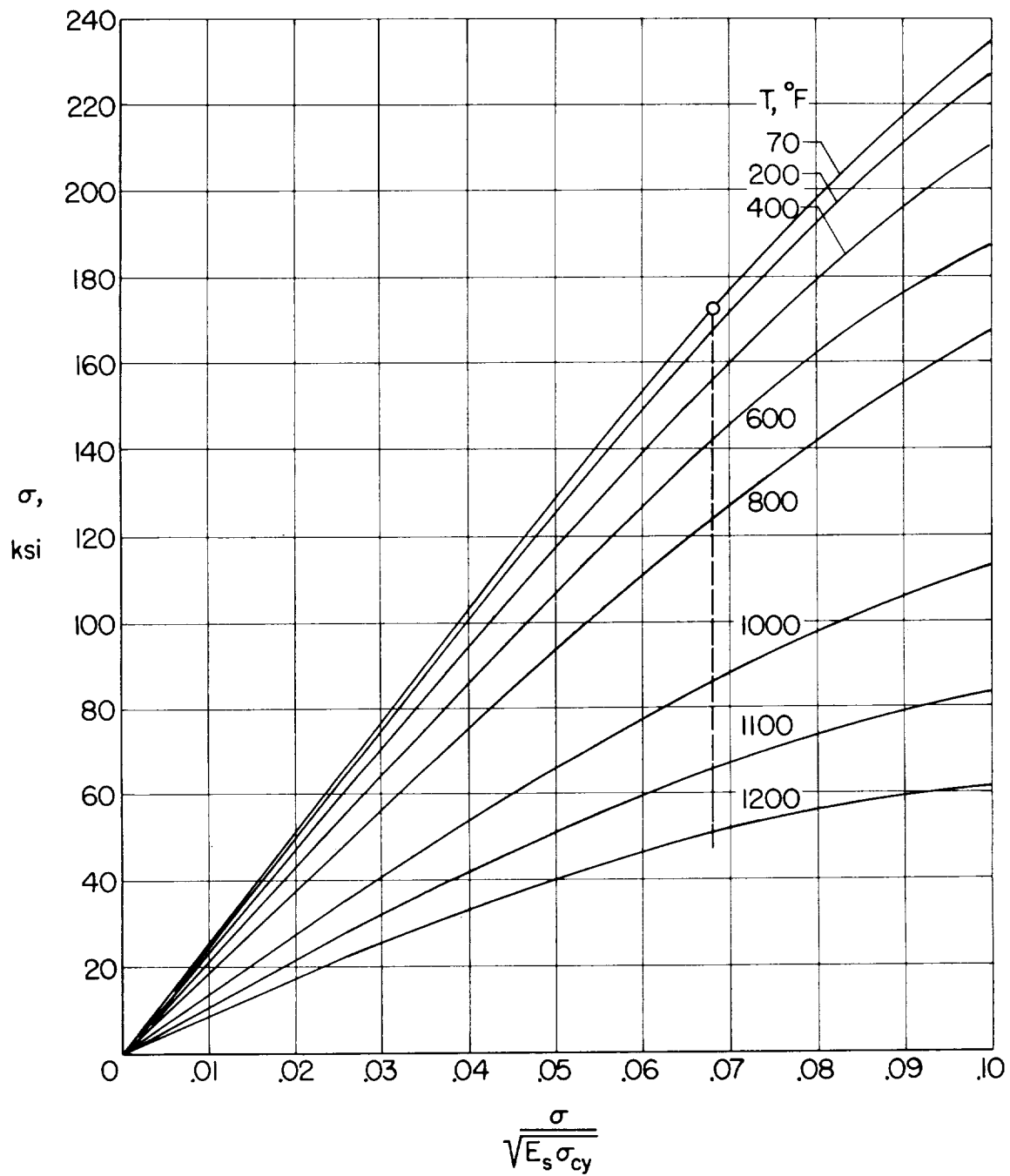
(a) Single-corrugated-core sandwiches of 17-7 PH stainless steel.

Figure 14.- Curves showing correlation procedure used to predict elevated-temperature crippling stresses from experimental room-temperature crippling stresses.



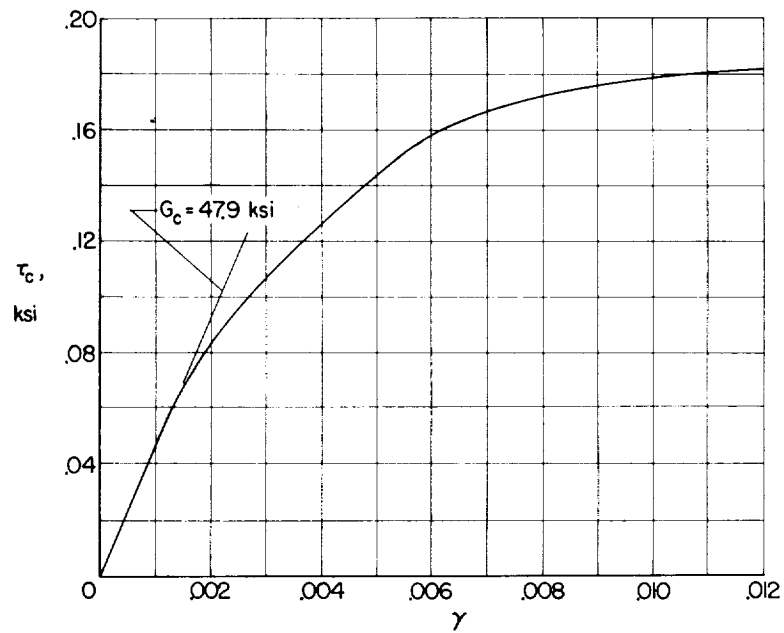
(b) Double-corrugated-core sandwiches of type 301 stainless steel weighing 1 pound per square foot.

Figure 14.- Continued.

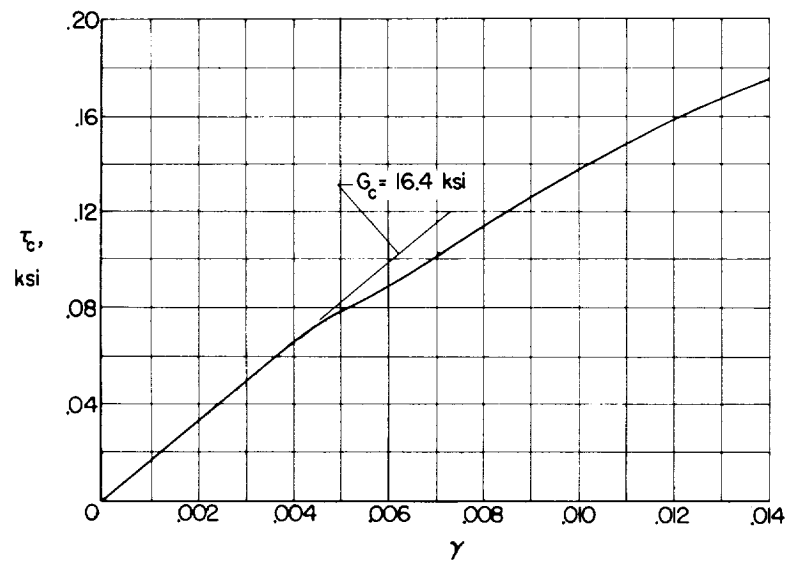


(c) Double-corrugated-core sandwiches of type 301 stainless steel weighing 2 pounds per square foot.

Figure 14.- Concluded.



(a) Square-cell core sandwiches.



(b) Hexagonal-cell core sandwiches.

Figure 15.- Curves of effective shear stress plotted against shear strain obtained from shear modulus tests of honeycomb cores at room temperature.

# NASA MEMO 6-2-59L

National Aeronautics and Space Administration.  
COMPRESSIVE STRENGTH OF STAINLESS-STEEL  
SANDWICHES AT ELEVATED TEMPERATURES.  
Eldon E. Mathauser and Richard A. Pride. June  
1959. 50p. diagrs., photos., tabs.  
(NASA MEMORANDUM 6-2-59L)

Experimental results are presented from crippling tests of specimens in the temperature range from 80° F to 1,200° F. The specimens included resistance-welded 17-7 PH stainless-steel sandwiches with single-corrugated cores, type 301 stainless-steel sandwiches with double-corrugated cores, and brazed 17-7 PH stainless-steel sandwiches with honeycomb cores. The experimental strengths are compared with predicted buckling and crippling strengths. Photographs of some of the tested specimens are included to show the modes of failure.

Copies obtainable from NASA, Washington

# NASA MEMO 6-2-59L

National Aeronautics and Space Administration.  
COMPRESSIVE STRENGTH OF STAINLESS-STEEL  
SANDWICHES AT ELEVATED TEMPERATURES.  
Eldon E. Mathauser and Richard A. Pride. June  
1959. 50p. diagrs., photos., tabs.  
(NASA MEMORANDUM 6-2-59L)

Experimental results are presented from crippling tests of specimens in the temperature range from 80° F to 1,200° F. The specimens included resistance-welded 17-7 PH stainless-steel sandwiches with single-corrugated cores, type 301 stainless-steel sandwiches with double-corrugated cores, and brazed 17-7 PH stainless-steel sandwiches with honeycomb cores. The experimental strengths are compared with predicted buckling and crippling strengths. Photographs of some of the tested specimens are included to show the modes of failure.

Copies obtainable from NASA, Washington

1. Loads and Stresses, Structural - Compression (4.3.7.2)
2. Sandwich and Laminates (5.1.11)
3. Materials, Properties - Compressive (5.2.2)
  - I. Mathauser, Eldon E.
  - II. Pride, Richard A.
  - III. NASA MEMO 6-2-59L

NASA

# NASA MEMO 6-2-59L

National Aeronautics and Space Administration.  
COMPRESSIVE STRENGTH OF STAINLESS-STEEL  
SANDWICHES AT ELEVATED TEMPERATURES.  
Eldon E. Mathauser and Richard A. Pride. June  
1959. 50p. diagrs., photos., tabs.  
(NASA MEMORANDUM 6-2-59L)

Experimental results are presented from crippling tests of specimens in the temperature range from 80° F to 1,200° F. The specimens included resistance-welded 17-7 PH stainless-steel sandwiches with single-corrugated cores, type 301 stainless-steel sandwiches with double-corrugated cores, and brazed 17-7 PH stainless-steel sandwiches with honeycomb cores. The experimental strengths are compared with predicted buckling and crippling strengths. Photographs of some of the tested specimens are included to show the modes of failure.

Copies obtainable from NASA, Washington

# NASA MEMO 6-2-59L

National Aeronautics and Space Administration.  
COMPRESSIVE STRENGTH OF STAINLESS-STEEL  
SANDWICHES AT ELEVATED TEMPERATURES.  
Eldon E. Mathauser and Richard A. Pride. June  
1959. 50p. diagrs., photos., tabs.  
(NASA MEMORANDUM 6-2-59L)

Experimental results are presented from crippling tests of specimens in the temperature range from 80° F to 1,200° F. The specimens included resistance-welded 17-7 PH stainless-steel sandwiches with single-corrugated cores, type 301 stainless-steel sandwiches with double-corrugated cores, and brazed 17-7 PH stainless-steel sandwiches with honeycomb cores. The experimental strengths are compared with predicted buckling and crippling strengths. Photographs of some of the tested specimens are included to show the modes of failure.

Copies obtainable from NASA, Washington

1. Loads and Stresses, Structural - Compression (4.3.7.2)
2. Sandwich and Laminates (5.1.11)
3. Materials, Properties - Compressive (5.2.2)
  - I. Mathauser, Eldon E.
  - II. Pride, Richard A.
  - III. NASA MEMO 6-2-59L

NASA

1. Loads and Stresses, Structural - Compression (4.3.7.2)
2. Sandwich and Laminates (5.1.11)
3. Materials, Properties - Compressive (5.2.2)
  - I. Mathauser, Eldon E.
  - II. Pride, Richard A.
  - III. NASA MEMO 6-2-59L

NASA

